Electronic Supplementary Information for

Understanding the Competition Between Hydrodechlorination and Friedel-Crafts Alkylation in PVC Dechlorination with Silylium Ions

Nicholas J. Roubineau,[a†] Eunice C. Castro,[a†] Kaustubh Rane,[b] Zachary A. Wood,[a] Angelyn N. Nguyen,[a] Nancy G. Bush,[a] Ayon Das,[a] Shaama Mallikarjun Sharada,[a,b*] Megan E. Fieser[a,c*]

[a]Department of Chemistry, University of Southern California, Los Angeles, CA 90089

[b]Mork Family Department of Chemical Engineering and Materials Science, University of Southern California, Los Angeles, CA 90089

[c]Wrigley Institute for Environment and Sustainability, University of Southern California, Los Angeles, CA 90089

[†]N.J.R. and E.C.C. contributed equally

Email: fieser@usc.edu

1. General Considerations

Most polymerization reactions were performed on the benchtop once conditions were optimized, unless noted otherwise. Any air-free polymerization reaction was set up in a nitrogen-containing glovebox before the reaction vessel is closed and the polymerization reaction is brought out of the glovebox and conducted closed in a fume hood. $[Ph_3C][B(C_6F_5)_4]$ was purchased from Fisher Chemical (Fisher, Product #: T28635G), anhydrous grade triethylsilane (Et_3SiH) (Aldrich. Product #: 230197) was purchased from Aldrich, and 1,1,3,3-tetramethyldisiloxane (TMDS) was purchased from Fischer Chemical and used as received. $[Ph_3C][B(C_6F_5)_4]$, anhydrous grade triethyl silane, benzene, toluene, ortho-, meta- and para-xylene were all stored and transferred out of the glovebox in a 20 mL scintillation vial to be properly used under benchtop conditions. All reagents were used within the same week of being brought out of the glovebox with the exception of the trityl borate lifetime studies in which the dried toluene, dried poly(vinyl chloride) (PVC), and Et_3SiH were all brought out on the same day of the reaction. "Low M_n" PVC (M_n = 43 kg/mol), M_n = 35 kg/mol PVC, and M_n = 99 kg/mol PVC purchased from Aldrich were readily available on benchtop and used as received. Mesitylene and TMDS were readily available on benchtop and used as received. NMR solvent $CDCl_3$ was purchased from Cambridge Isotope Laboratories and used as received. Product yields for the synthesized vinyl aromatic copolymers were estimated using the following theoretical yield formula: mmolPVC x $\{(mol\%_{PVC} \times MW_{PVC}) + (mol\%_{PE} \times MW_{PE}) + mol\%_{P\text{“}A\text{”}} \times MW_{P\text{“}A\text{”}})\}$.

To calculate:

mol%P"A" -

$$PE_{\text{relative amount}} = \frac{(PE_{int} - (PVC_{int} \times 2)) - (\#\text{ of H unaccounted for in PA unit})}{4}$$

$$\text{mol \% P'A'} = \frac{1}{1 + PVC_{int} + PE_{\text{relative amount}}} \times 100$$

mol%PE -

$$PE_{\text{relative amount}} = \frac{(PE_{int} - (PVC_{int} \times 2)) - (\#\text{ of H unaccounted for in PA unit})}{4}$$

$$\text{mol \% PE} = \frac{\text{PE}_{\text{relative amount}}}{1+\text{PVC}_{\text{int}}+\text{PE}_{\text{relative amount}}} \text{ x } 100$$

mol % P"VC = 100 - (mol% PE + mol% P'A')

Where “A” is the aromatic solvent being used.

1.1. Methods

^{1}H nuclear magnetic resonance (NMR) spectra were recorded on a Varian Mercury 400 Magnetic Resonance Spectrometer and referenced to residual solvent resonances. Thermogravimetric analysis (TGA) data were collected using a Mettler-Toledo STARe System TGA/DSC3+ with a heating rate of 10 °C/min. Fourier Transform Infrared Spectroscopy (FT-IR) data was collected using an Agilent Cary 630 FTIR spectrometer equipped with a single reflection diamond (Di) attenuated total reflectance (ATR) module. DSC traces were recorded using a TA Instruments Discovery DSC 250 Auto, equipped with a Discovery LN_2 Pump, and processed with TRIOS software. The DSC measurements were made at a heating rate of 10 °C/min and N_2 flow rate of 20 ml/min, and T_g values were obtained from the peak of the glass transition in the second heating curve. No T_m values were observed.

DFT calculations are performed using the quantum chemistry software Q-Chem[1] at ωB97X-D/def2-SVP[2,3] level of theory. These calculations employ the conductor-like polarizable continuum model (C-PCM) for implicit solvation to capture the effect of the solvent THF (dielectric constant = 7.58).[4-6] The minima are verified using the vibrational analysis and the free energies computed using the rigid rotor harmonic oscillator approximation at 298K.[7] 1,3,5,7-tetrachloroheptane is chosen as the model PVC system which is dechlorinated by triethylsilane (TES). This computational study investigates the relative thermodynamic feasibilities of competing hydrodechlorination, Friedel-Crafts (FC) alkylation, and polyindene formation reactions.

2. General Procedures for Hydrodechlorination and Friedel Crafts Alkylation of PVC

2.1. Optimized benchtop synthesis of Poly(ethylene-co-toluene) (Table 1, Entry 1, 4-6. Table S1)

$[Ph_3C][B(C_6F_5)_4]$ (5.0 mg, 0.005 mmol, 0.25 mol%), Et_3SiH (0.52 mL, 3.26 mmol, 1.5 equiv), dry toluene (2.53 mL, 23.9 mmol, 11 equiv) (all previously stored under N_2 atmosphere in a glovebox) and a stir bar were transferred into a 2 dram vial equipped with an aluminum lined cap. The mixture was allowed to stir for 5 minutes at room temperature before being pipetted into another 2-dram vial, equipped with a Teflon coated cap, that contained pre-weighed low molecular weight PVC (136.0 mg, 2.18 mmol, 1 equiv). The vial was then sealed with electrical tape and, immediately after, placed inside a Chemglass high-throughput tray that was preheated at 110 °C. After stirring at 600 rpm for 30 minutes, the reaction mixture was transferred into a 20 mL scintillation vial and then quenched with isopropanol (~15 mL), which resulted in the precipitation of white solids. The solids were left to settle overnight before decanting the supernatant and drying under vacuum at 80 °C overnight.

2.2. Studying the stability of $[Ph_3C][B(C_6F_5)_4]$ (Table S2)

$[Ph_3C][B(C_6F_5)_4]$ was first stored outside the desiccator for up to 71 days. On each dedicated day of the reaction, Et_3SiH, dried toluene, and dried low molecular PVC were all transferred outside of the glovebox before being weighed and prepared on the benchtop. $[Ph_3C][B(C_6F_5)_4]$ (5.0 mg, 0.005 mmol, 0.25 mol%), Et_3SiH (0.52 mL, 3.26 mmol 1.5 equiv), toluene (2.53 mL, 23.9 mmol 11 equiv), and a stir bar were first transferred into a 2-dram vial equipped with an aluminum lined cap. The mixture was then allowed to stir for approximately 5 minutes before being pipetted into another 2-dram vial with a Teflon-coated cap that contained the dried low molecular weight PVC (136.0 mg, 2.18 mmol, 1 equiv). Note that the dried PVC was also weighed on the benchtop. The vial was then sealed with electrical tape and, immediately after, placed on a Chemglass high-throughput tray preheated at 110°C. After stirring at 600 rpm for 30 minutes, the reaction mixture was transferred into a 20 mL scintillation vial and quenched with isopropanol (15 mL), which resulted in the precipitation of white solids. The solids were left to settle overnight before the supernatant was decanted. An alternative and quicker process is to centrifuge the solution before decanting

the supernatant. Prior to characterization, the polymer was also dried at approximately 80 °C over 14 hours under dynamic vacuum.

2.3 Benchtop Synthesis of poly(ethylene-co-toluene) – Studying the effects of the slow addition of Et_3SiH (Table 1, Entry 2. Table S3, Entry 5a-5b)

An addition funnel was first prepared with a mixture of Et_3SiH (0.42 mL, 2.63 mmol, 1.2 equiv) and toluene (2.00 mL, 18.9 mmol, 8.7 equiv). $[Ph_3C][B(C_6F_5)_4]$ (5.0 mg, 0.005 mmol, 0.25 mol%), toluene (2.53 mL, 23.9 mmol, 11 equiv), Et_3SiH (0.05 mL, 0.313 mmol, 0.15 equiv), and a stir bar were first transferred into a 2 dram vial equipped with an aluminum lined cap. The mixture was then allowed to stir for 5 minutes before pipetted into a 50 mL round bottom flask containing pre-weighed low molecular weight PVC (136.0 mg, 2.18 mmol, 1 equiv). The round bottom flask was then secured onto the addition funnel and, immediately after, lowered into an oil bath that was preheated at 60 °C. The Et_3SiH in the separatory funnel was then added in a slow and constant stream over 10 minutes. After adding all of the Et_3SiH, the reaction mixture was left to stir for 2 hours before being quenched with isopropanol (15 mL). This resulted in the precipitation of white solids. The solids were left to settle for several hours before decanting the supernatant. Prior to characterization, the polymer was also dried at approximately 80 °C over 14 hours under dynamic vacuum.

2.4 Benchtop Synthesis of poly(ethylene-co-toluene) – Studying the effects of increasing toluene equivalents (Table 1, Entry 3. Table S3, Entry 6a-6b)

$[Ph_3C][B(C_6F_5)_4]$ (5.0 mg, 0.005 mmol, 0.25 mol%), Et_3SiH (0.52 mL, 3.26 mmol, 1.5 equiv), toluene (5.06 mL, 47.9 mmol, 22 equiv), and a stir bar were transferred into a 2 dram vial equipped with an aluminum lined cap. The mixture was then allowed to stir for approximately 5 minutes before being pipetted into another 2-dram vial, equipped with a Teflon-coated cap, that contained low molecular weight PVC (136.0 mg, 2.18 mmol, 1 equiv). The vial was then sealed with electrical tape and, immediately after, placed on a Chemglass high-throughput tray preheated at 110°C. After stirring at 600 rpm for 18 hours, the reaction mixture was transferred into a 20 mL scintillation vial and then quenched with isopropanol (15 mL), which resulted in the precipitation of white solids. The solids were left to settle overnight before decanting the

supernatant. An alternative and quicker process is to centrifuge the solution before decanting the supernatant. Prior to characterization, the polymer was also dried at approximately 80 °C over 14 hours under dynamic vacuum.

2.5. Synthesis of Poly(ethylene-co-toluene) Using TMDS (Table 2. Table S4)

$[Ph_3C][B(C_6F_5)_4]$ (5.0 mg, 0.005 mmol, 0.25 mol%), TMDS (0.21-0.58 mL, 1.20-3.26 mmol, 0.55-1.5 equiv), toluene stored on the benchtop (2.53 mL, 23.9 mmol, 11 equiv) and a stir bar were transferred into a 2 dram vial equipped with an aluminum lined cap. The mixture was allowed to stir for 5 minutes at room temperature before being pipetted into another 2-dram vial, equipped with a Teflon coated cap, that contained pre-weighed low molecular weight PVC (136.0 mg, 2.18 mmol, 1 equiv). The vial was then sealed with electrical tape and, immediately after, placed inside a Chemglass high-throughput tray that was preheated at 110 °C. After stirring at 600 rpm for 30 minutes, the reaction mixture was transferred into a 20 mL scintillation vial and then quenched with isopropanol (~15 mL), which resulted in the precipitation of white solids. The solids were left to settle overnight before decanting the supernatant and drying under vacuum at 80 °C overnight.

2.6 Synthesis of Poly(ethylene-co-o-xylene) (Table S5)

Reaction was performed following similar procedure as that for poly(ethylene-co-toluene), in which the volume of ortho-xylene was kept constant, thus the equivalents were lower (2.53 mL, 20.9 mmol, 9.6 equiv).

2.7 Synthesis of Poly(ethylene-co-m-xylene) (Table S6)

Reaction was performed following similar procedure as that for poly(ethylene-co-toluene), in which the volume of meta-xylene was kept constant, thus the equivalents were lower (2.53 mL, 20.7 mmol, 9.5 equiv).

2.8 Synthesis of Poly(ethylene-co-p-xylene) (Table S7)

Reaction was performed following similar procedure as that for poly(ethylene-co-toluene), in which the volume of para-xylene was kept constant, thus the equivalents were lower (2.53 mL, 20.5 mmol, 9.4 equiv).

2.9 Synthesis of Poly(ethylene-co-benzene) (Table S8)

Reaction was performed following similar procedure as that for poly(ethylene-co-toluene), in which the volume of benzene was kept constant, thus the equivalents were higher (2.53 mL, 28.3 mmol, 13 equiv).

2.10 Synthesis of Poly(ethylene-co-benzene) – prepared airfree with higher catalyst loading (Table S8, Entry 1a-1b)

$[Ph_3C][B(C_6F_5)_4]$ (10.0 mg, 0.011 mmol, 0.5 mol%), Et_3SiH (0.52 mL, 3.26 mmol, 1.5 equiv), dry benzene (2.53 mL, 28.3 mmol, 13 equiv) and a stir bar were transferred into a 2 dram vial equipped with an aluminum lined cap. The mixture was allowed to stir for 5 minutes at room temperature before being pipetted into another 2-dram vial, equipped with a Teflon coated cap, that contained pre-weighed low molecular weight PVC (136.0 mg, 2.18 mmol, 1 equiv). Previous steps performed under N_2 atmosphere in a glovebox. The vial was then sealed with electrical tape and, immediately after, placed inside a Chemglass high-throughput tray that was preheated at 110 °C. After stirring at 600 rpm for 30 minutes, the reaction mixture was transferred into a 20 mL scintillation vial and then quenched with isopropanol (~15 mL), which resulted in the precipitation of white solids. The solids were left to settle overnight before decanting the supernatant and drying under vacuum at 80 °C overnight.

2.11 Synthesis of Poly(ethylene-co-mesitylene) (Table S9)

$[Ph_3C][B(C_6F_5)_4]$ (5.0 mg, 0.005 mmol, 0.25 mol%) (previously stored under N_2 atmosphere in a glovebox), Et_3SiH (0.52 mL, 3.26 mmol, 1.5 equiv) and mesitylene (2.53 mL, 18.2 mmol, 8.4 equiv) (both from the benchtop) and a stir bar were transferred into a 2 dram vial equipped with an aluminum lined cap. The mixture was allowed to stir for 5 minutes at room temperature before being pipetted into another 2-dram vial, equipped with a Teflon coated cap, that contained pre-weighed low molecular weight PVC (136.0 mg, 2.18 mmol, 1 equiv). The vial was then sealed with electrical tape and, immediately after, placed inside a Chemglass high-throughput tray that was preheated at 110 °C. After stirring at 600 rpm for 30 minutes, the reaction mixture was transferred into a 20 mL scintillation vial and then quenched with isopropanol (~15

mL), which resulted in the precipitation of white solids. The reaction mixture was then cooled to 0°C, centrifuged, and the supernatant was decanted. The were dried under vacuum at 80 °C overnight.

2.12 Synthesis of Poly(ethylene-co-mesitylene) – higher catalyst loading (Table S9, Entry 3a-3b)

$[Ph_3C][B(C_6F_5)_4]$ (10.0 mg, 0.011 mmol, 0.5 mol%) (previously stored under N_2 atmosphere in a glovebox), Et_3SiH (0.52 mL, 3.26 mmol, 1.5 equiv) and mesitylene (2.53 mL, 18.2 mmol, 8.4 equiv) (both from the benchtop) and a stir bar were transferred into a 2 dram vial equipped with an aluminum lined cap. The mixture was allowed to stir for 5 minutes at room temperature before being pipetted into another 2-dram vial, equipped with a Teflon coated cap, that contained pre-weighed low molecular weight PVC (136.0 mg, 2.18 mmol, 1 equiv). The vial was then sealed with electrical tape and, immediately after, placed inside a Chemglass high-throughput tray that was preheated at 110 °C. After stirring at 600 rpm for 30 minutes, the reaction mixture was transferred into a 20 mL scintillation vial and then quenched with isopropanol (~15 mL), which resulted in the precipitation of white solids. The reaction mixture was then cooled to 0°C, centrifuged, and the supernatant was decanted. The were dried under vacuum at 80 °C overnight.

2.13 Synthesis of Poly(ethylene-co-toluene) from 35 kg/mol PVC (Table S10, Entry 1a-3b)

Reaction was performed following similar procedure as that for poly(ethylene-co-toluene) using 43 kg/mol PVC.

2.14 Synthesis of Poly(ethylene-co-toluene) from 99 kg/mol PVC (Table S10, Entry 4a-5b)

Reaction was performed following similar procedure as that for poly(ethylene-co-toluene) using 99 kg/mol PVC.

2.15 Synthesis of Poly(ethylene-co-toluene) from 99 kg/mol PVC – higher catalyst and silane loading (Table S10, Entry 6a-6b)

$[Ph_3C][B(C_6F_5)_4]$ (10.0 mg, 0.011 mmol, 0.5 mol%), Et_3SiH (0.69 mL, 4.4 mmol, 2.0 equiv), dry toluene (2.53 mL, 23.9 mmol, 11 equiv) (all previously stored under N_2 atmosphere in a glovebox) and a stir bar were transferred into a 2 dram vial equipped with an aluminum lined cap. The mixture was allowed to stir for 5 minutes at room temperature before being pipetted into another 2-dram vial, equipped with a Teflon coated cap, that contained pre-weighed 99 kg/mol PVC (136.0 mg, 2.18 mmol, 1 equiv). The vial was then

sealed with electrical tape and, immediately after, placed inside a Chemglass high-throughput tray that was preheated at 110 °C. After stirring at 600 rpm for 30 minutes, the reaction mixture was transferred into a 20 mL scintillation vial and then quenched with isopropanol (~15 mL), which resulted in the precipitation of white solids. The solids were left to settle overnight before decanting the supernatant and drying under vacuum at 80 °C overnight.

3. Tabulated Reaction Data

Table S1 Optimization of silylium catalyzed dechlorination of PVC on the benchtop

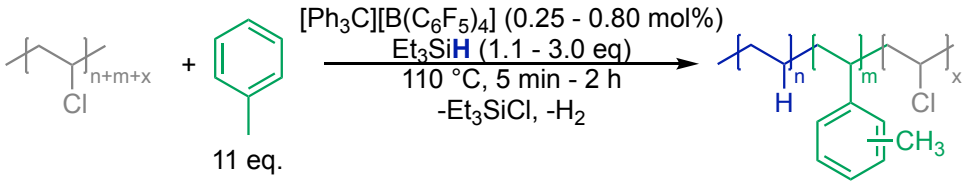

Entry	$[Ph_3C][B(C_6F_5)_4]$ loading (mol %)[a]	Et_3SiH (eq)[b]	Time (min)	PE mol%[c]	Aryl mol%[c]	PVC mol%[c]	Variation from Standard
1	0.25	1.1	5	70	18	12	None
2	0.25	1.1	5	58	17	25	Air-exposed
3	0.25	1.1	120	75	19	6	Air-exposed, longer time (2 h)
4	0.80	1.1	120	76	14	10	Air-exposed, higher initiator loading (0.8 mol%), longer time (2 h)
5	0.25	1.1	5	77	22	1	Air-exposed, dried toluene
6	0.25	3.0	120	82	18	0	Air-exposed, higher silane amount (3 eq.), longer time (2 h)
7	0.25	1.5	30	79	21	0	Air-exposed, dried toluene, longer time (30 min), higher silane amount (1.5 eq.)

[a]Initiator mol% relative to moles of PVC. [b]Et_3SiH equivalence relative to PVC. [c]Calculated from ^1H NMR spectra taken in $CDCl_3$.

Table S2 Probing the benchtop stability of the catalyst

Entry[a]	# of days $[Ph_3C][B(C_6F_5)_4]$ is stored on benchtop	Aryl mol %[b]	PE mol %[b]
1	0	20	80
2	1	20	80
3	3	19	81
4	7	19	81
5	14	18	82
6	30	13	87
7	71	20	80

[a]30-minute reactions were performed with 0.25 mol% of the catalyst and 1.5eq of Et_3SiH at 110°C using dried toluene as the aromatic solvent. Initiator mol% relative to moles of PVC. Et_3SiH equivalence relative to PVC. [b]Calculated from ^1H NMR spectra taken in $CDCl_3$.

Table S3 Additional replicate runs of PVC to poly(ethylene-co-toluene)

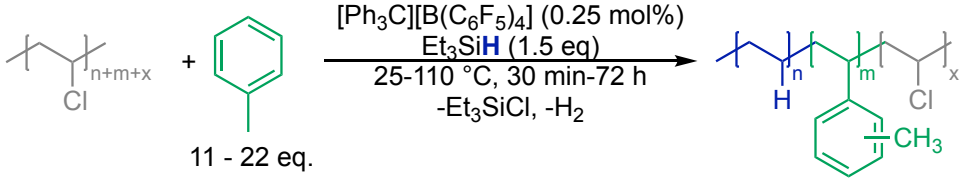

Entry[a]	Reaction time (h)	Temp (°C)	PE mol %[b]	Aryl mol %[b]	PVC mol %[b]	T_g (°C)[c]
1a	0.5	110	79	21	0	69
1b	0.5	110	81	19	0	79
2a	1	80	79	21	0	83
2b	1	80	83	17	0	-
2c	1	80	80	20	0	79
3a	1	60	79	21	0	91
3b	1	60	78	22	0	-
3c	1	60	81	19	0	81
4a	72	25	85	16	0	112
4b	72	25	86	14	0	-
4c	72	25	80	20	0	106
5a[d]	2	110	42	13	45	-
5b[d]	2	110	54	10	36	-
6a[e]	18	110	78	22	0	80
6b[e]	18	110	79	21	0	-

[a]Reactions were performed with 0.25 mol% of the catalyst, Et_3SiH at 110°C using dried toluene as the aromatic solvent. Initiator mol% relative to moles of PVC. Et_3SiH equivalence relative to PVC. [b]Calculated from ^1H NMR spectra taken in $CDCl_3$. [c]Glass transition peak in second heating curve of DSC. [d]Silane was added slowly throughout the reaction. [e]22 equiv. toluene was used.

Table S4 Additional replicate runs using TMDS as silane source

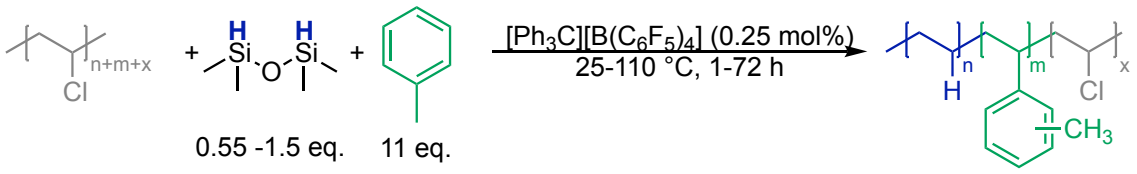

Entry[a]	TMDS eq.	Reaction time (h)	Temp (°C)	PE mol%[b]	Aryl mol%[b]	PVC mol%[b]	T_g (°C)[c]
1a	0.75	1	110	25	17	58	-
1b	0.75	1	110	49	16	35	-
2a	1	1	110	74	24	2	-
2b	1	1	110	79	21	0	69
3a	1.1	1	110	78	22	0	74
3b	1.1	1	110	77	23	0	-
4a	1.5	1	110	77	23	0	72
4b	1.5	1	110	78	22	0	-
4c	1.5	1	110	78	22	0	-
5	1.1	1	60	78	22	0	88
6	1.1	72	25	82	18	0	101
7	0.55	22	110	44	13	43	-
8	0.55	1	110	39	11	50	-
9	0.55	1	60	45	16	41	-
10	0.55	2	60	34	11	55	-
11	0.55	6	60	43	13	44	-
12	0.55	18	60	39	12	49	-

[a]Reactions were performed using low molecular weight PVC with 0.25 mol% of the catalyst and 0.55-1.5 equivalents of TMDS in benchtop toluene as the aromatic solvent. [b]Calculated from ^{1}H NMR spectra taken in $CDCl_3$. [c]Glass transition peak in second heating curve of DSC.

Table S5 Conversion of PVC to poly(ethylene-co-o-xylene)

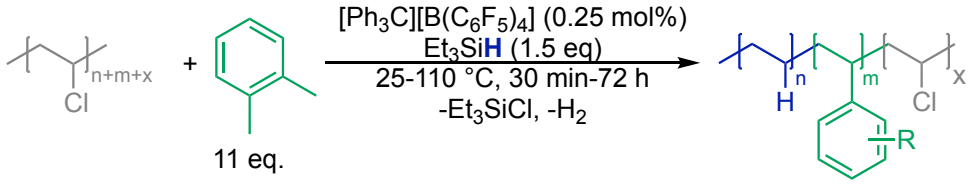

Entry[a]	Reaction time	Temp (°C)	PE mol%[b]	Aryl mol%[b]	PVC mol%[b]	T_g (°C)[c]
1a	30 min	110	79	21	0	65
1b	30 min	110	80	20	0	-
1c	30 min	110	80	20	0	79
2a	1 h	60	78	22	0	76
2b	1 h	60	77	23	0	80
2c	1 h	60	77	23	0	-
3a	72 h	25	79	21	0	85
3b	72 h	25	78	22	0	-
3c	72 h	25	77	23	0	87

[a]Reactions were performed using low molecular weight PVC with 0.25 mol% of the catalyst and 1.5 equivalents of Et_3SiH in dried ortho-xylene as the aromatic solvent. [b]Calculated from ^1H NMR spectra taken in $CDCl_3$. [c]Glass transition peak in second heating curve of DSC.

Table S6 Conversion of PVC to poly(ethylene-co-m-xylene)

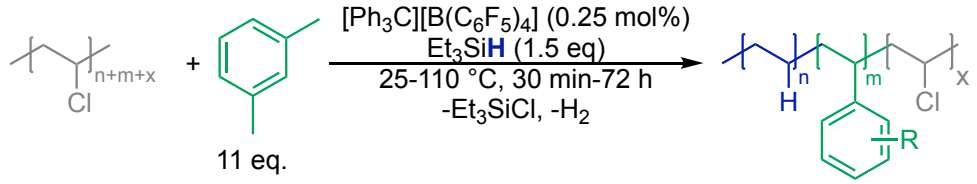

Entry[a]	Reaction time	Temp (°C)	PE mol%[b]	Aryl mol%[b]	PVC mol%[b]	T_g (°C)[c]
1a	30 min	110	81	19	0	69
1b	30 min	110	80	20	0	-
1c	30 min	110	80	20	0	77
2a	1 h	60	81	19	0	78
2b	1 h	60	79	21	0	-
2c	2 h	60	80	20	0	75
3a	72 h	25	78	22	0	77
3b	72 h	25	77	23	0	-
3c	72 h	25	87	13	0	90

[a]Reactions were performed using low molecular weight PVC with 0.25 mol% of the catalyst and 1.5 equivalents of Et_3SiH in dried meta-xylene as the aromatic solvent. [b]Calculated from ^1H NMR spectra taken in $CDCl_3$. [c]Glass transition peak in second heating curve of DSC.

Table S7 Conversion of PVC to poly(ethylene-co-p-xylene)

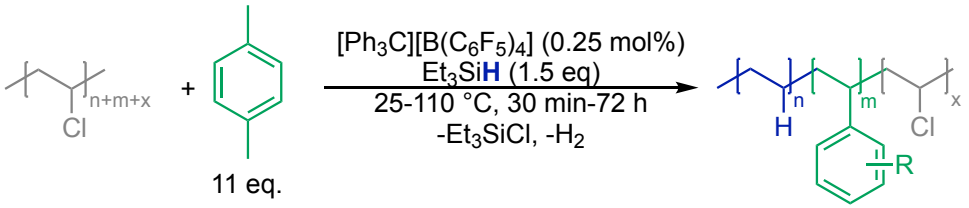

Entry[a]	Reaction time	Temp (°C)	PE mol%[b]	Aryl mol%[b]	PVC mol%[b]	T_g (°C)[c]
1a	30 min	110	84	16	0	60
1b	30 min	110	83	17	0	71
2a	5 h	60	84	16	0	80
2b	5 h	60	83	17	0	93
2c	5 h	60	83	17	0	-
3a	72 h	25	86	14	0	108
3b	72 h	25	90	10	0	108

[a]Reactions were performed using low molecular weight PVC with 0.25 mol% of the catalyst and 1.5 equivalents of Et_3SiH in dried para-xylene as the aromatic solvent. [b]Calculated from ^1H NMR spectra taken in $CDCl_3$. [c]Glass transition peak in second heating curve of DSC.

Table S8 Conversion of PVC to poly(ethylene-co-benzene)

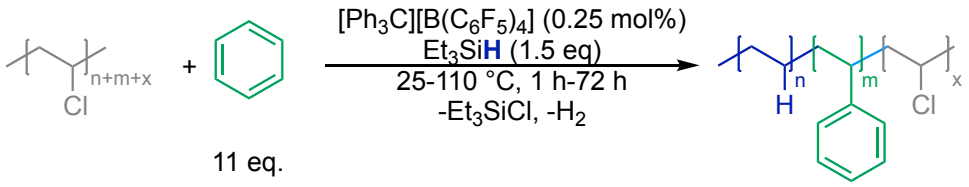

Entry[a]	Reaction time (h)	Temp (°C)	PE mol%[b]	Aryl mol%[b]	PVC mol%[b]	T_g (°C)[c]
1a[d]	1	110	86	14	0	70
1b[d]	1	110	87	13	0	79
2a	1	60	88	12	0	103
2b	1	60	88	12	0	91
3a	72	25	89	11	0	124
3b	72	25	91	9	0	125

[a]Reactions were performed using low molecular weight PVC with 0.25 mol% of the catalyst and 1.5 equivalents of Et_3SiH in dried benzene as the aromatic solvent. [b]Calculated from ^1H NMR spectra taken in $CDCl_3$. [c]Glass transition peak in second heating curve of DSC. [d]Reaction prepared in glovebox, performed in N2 atomosphere. 0.5 mol% of catalyst was used instead of 0.25 mol%.

Table S9 Conversion of PVC to poly(ethylene-co-mesitylene)

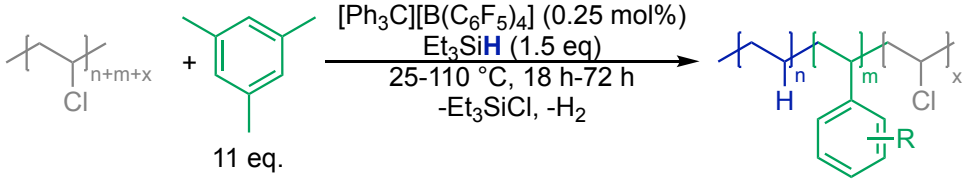

Entry[a]	Reaction time (h)	Temp (°C)	PE mol%[b]	Aryl mol%[b]	PVC mol%[b]	T_g (°C)[c]
1a	18	110	88	12	0	52
1b	18	110	88	12	0	49
2a	18	60	86	14	0	64
2b	18	60	87	13	0	63
3a[d]	72	25	86	14	0	73
3b[d]	72	25	85	15	0	77

[a]Reactions were performed using low molecular weight PVC with 0.25 mol% of the catalyst and 1.5 equivalents of Et_3SiH in dried benzene as the aromatic solvent. [b]Calculated from ^1H NMR spectra taken in $CDCl_3$. [c]Glass transition peak in second heating curve of DSC. [d]0.5 mol% of catalyst was used instead of 0.25 mol%

Table S10 Conversion of PVC to poly(ethylene-co-toluene) from different MW PVC substrates

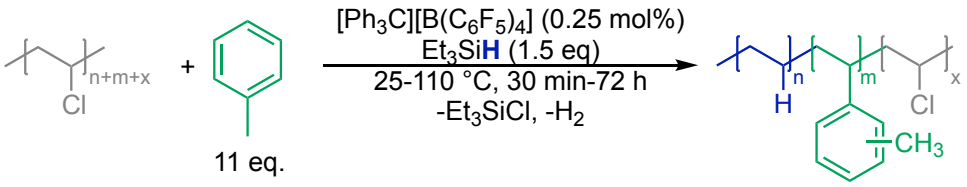

Entry[a]	Reaction time	Temp (°C)	PVC substrate	PE mol%[b]	Aryl mol%[b]	PVC mol%[b]	T_g (°C)[c]
1a	30 min	110	35 kg/mol	81	19	0	81
1b	30 min	110	35 kg/mol	80	20	0	77
2a	1 h	60	35 kg/mol	83	17	0	91
2b	1 h	60	35 kg/mol	79	21	0	93
3a	72 h	25	35 kg/mol	81	19	0	102
3b	72 h	25	35 kg/mol	79	21	0	106
4a	30 min	110	99 kg/mol	83	17	0	59
4b	30 min	110	99 kg/mol	80	20	0	64
5a	2 h	60	99 kg/mol	79	21	0	102
5b	2 h	60	99 kg/mol	79	21	0	97
6a[d]	72 h	25	99 kg/mol	92	8	0	123
6b[d]	72 h	25	99 kg/mol	92	8	0	116

[a]Reactions were performed using desired PVC substrate with 0.25 mol% of the catalyst and 1.5 equivalents of Et_3SiH in dried toluene as the aromatic solvent. [b]Calculated from ^1H NMR spectra taken in $CDCl_3$. [c]Glass transition peak in second heating curve of DSC. [d]0.5 mol% of catalyst and 2.0 equiv of Et_3SiH were used instead of 0.25 mol% and 1.5 equiv, respectively.

4. ^{1}H NMR Data

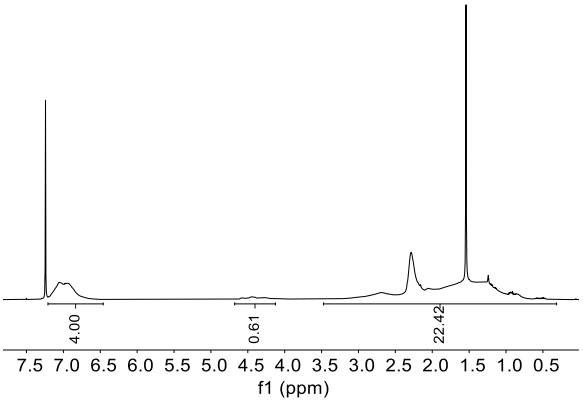

Fig. S1 ^{1}H NMR spectrum in $CDCl_3$ of poly(vinyl chloride-co-ethylene-co-toluene) product in Table S1, Entry 1

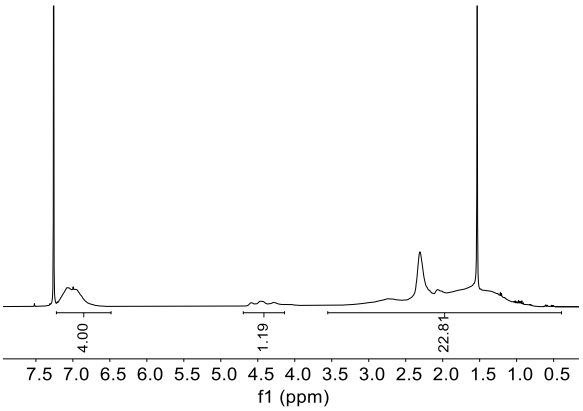

Fig. S2 ^{1}H NMR spectrum in $CDCl_3$ of poly(vinyl chloride-co-ethylene-co-toluene) product in Table S1, Entry 2

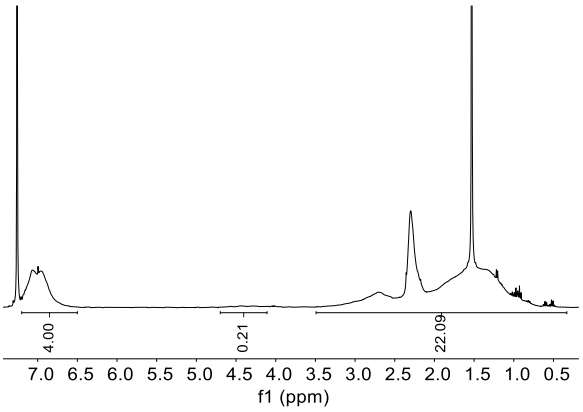

Fig. S3 ^{1}H NMR spectrum in $CDCl_3$ of poly(vinyl chloride-co-ethylene-co-toluene) product in Table S1, Entry 3

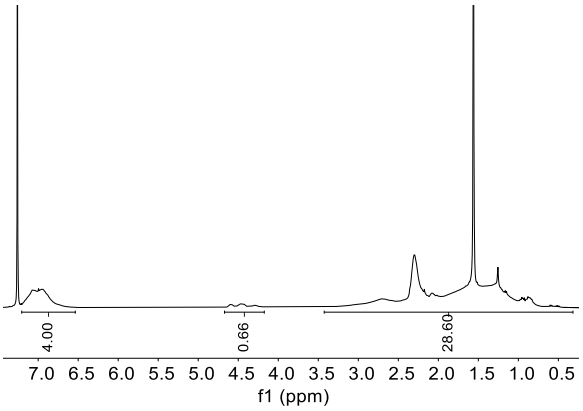

Fig. S4 ^{1}H NMR spectrum in $CDCl_3$ of poly(vinyl chloride-co-ethylene-co-toluene) product in Table S1, Entry 4 and Table S3, Entry 1a

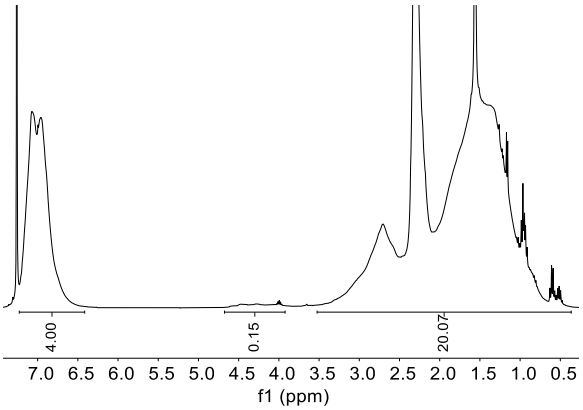

Fig. S5 ^{1}H NMR spectrum in $CDCl_3$ of poly(vinyl chloride-co-ethylene-co-toluene) product in Table S1, Entry 5

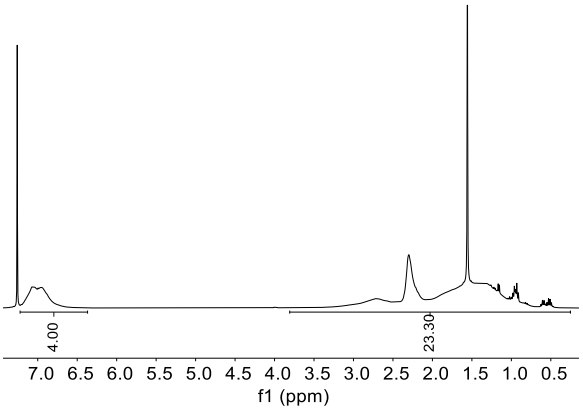

Fig. S6 ^{1}H NMR spectrum in $CDCl_3$ of poly(ethylene-co-toluene) product in Table S1, Entry 6

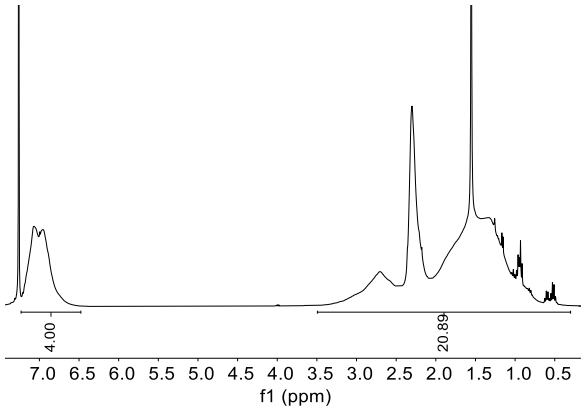

Fig. S7 ^{1}H NMR spectrum in $CDCl_3$ of poly(ethylene-co-toluene) product in Table S1, Entry 7

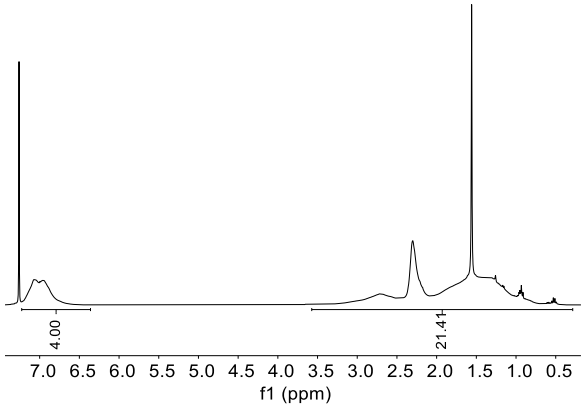

Fig. S8 ^{1}H NMR spectrum in $CDCl_3$ of poly(ethylene-co-toluene) product in Table S2, Entry 1

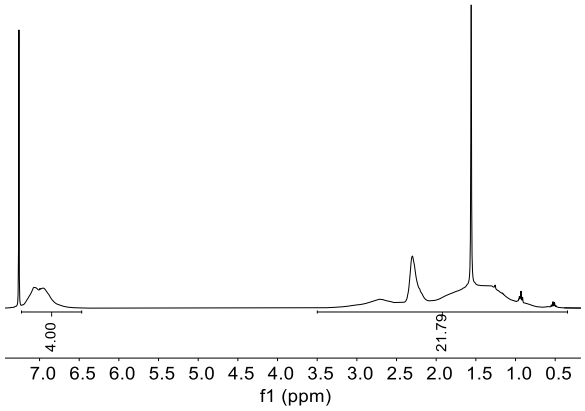

Fig. S9 ^{1}H NMR spectrum in $CDCl_3$ of poly(ethylene-co-toluene) product in Table S2, Entry 2

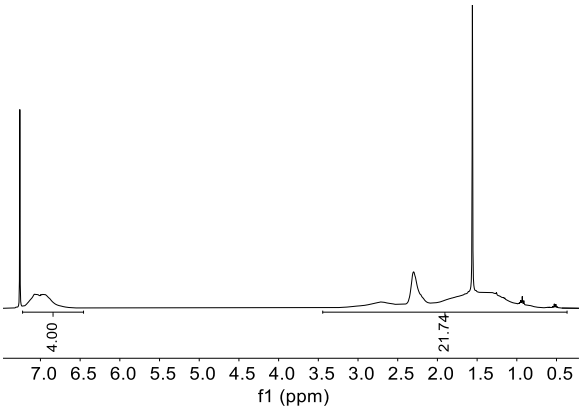

Fig. S10 ^{1}H NMR spectrum in $CDCl_3$ of poly(ethylene-co-toluene) product in Table S2, Entry 3

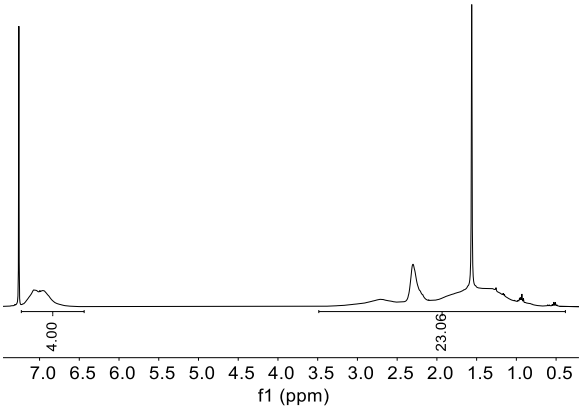

Fig. S11 ^{1}H NMR spectrum in $CDCl_3$ of poly(ethylene-co-toluene) product in Table S2, Entry 4

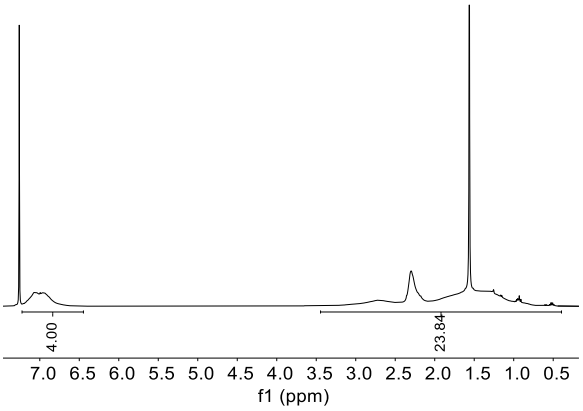

Fig. S12 ^{1}H NMR spectrum in $CDCl_3$ of poly(ethylene-co-toluene) product in Table S2, Entry 5

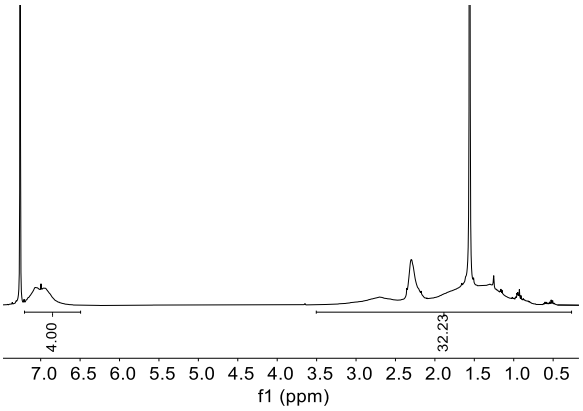

Fig. S13 ^{1}H NMR spectrum in $CDCl_3$ of poly(ethylene-co-toluene) product in Table S2, Entry 6

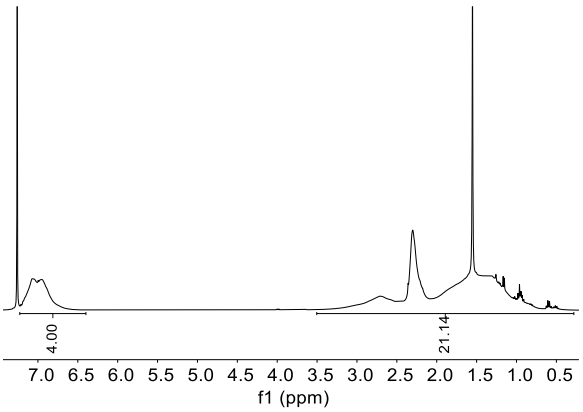

Fig. S14 ^{1}H NMR spectrum in $CDCl_3$ of poly(ethylene-co-toluene) product in Table S2, Entry 7

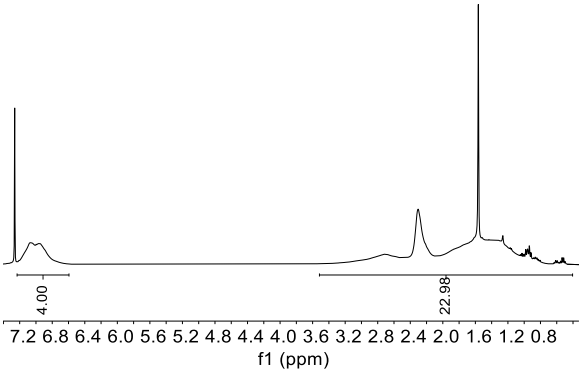

Fig. S15 ^{1}H NMR spectrum in $CDCl_3$ of poly(ethylene-co-toluene) product in Table S3, Entry 1b

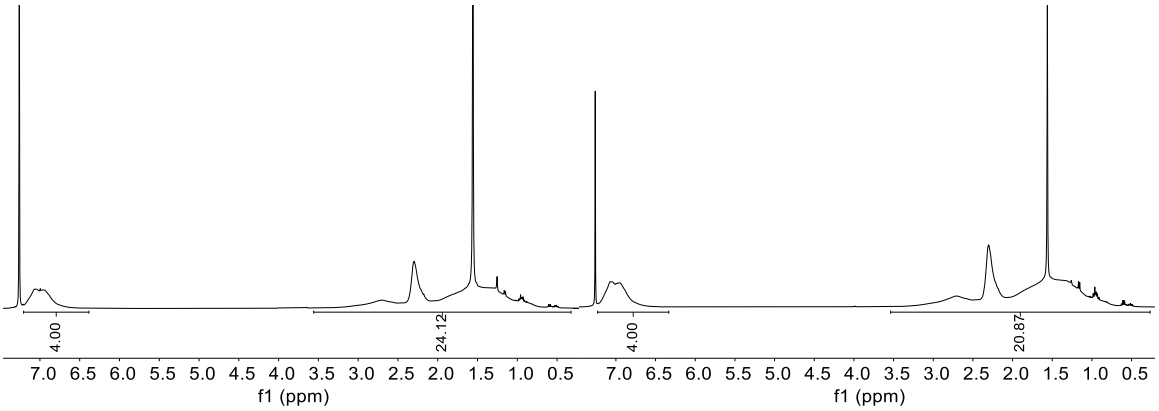

Fig. S16 ^{1}H NMR spectrum in $CDCl_3$ of poly(ethylene-co-toluene) product in Table S3, Entry 2a (left) and 2b (right)

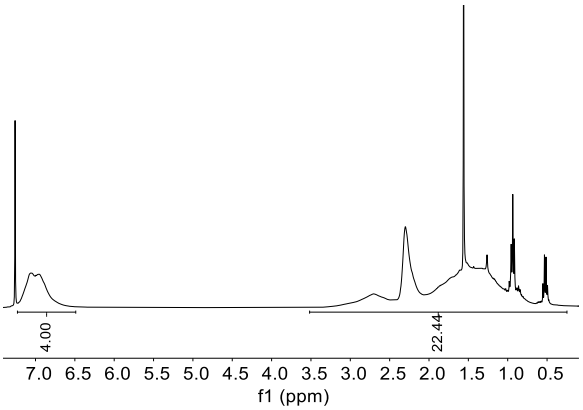

Fig. S17 ^{1}H NMR spectrum in $CDCl_3$ of poly(ethylene-co-toluene) product in Table S3, Entry 2c

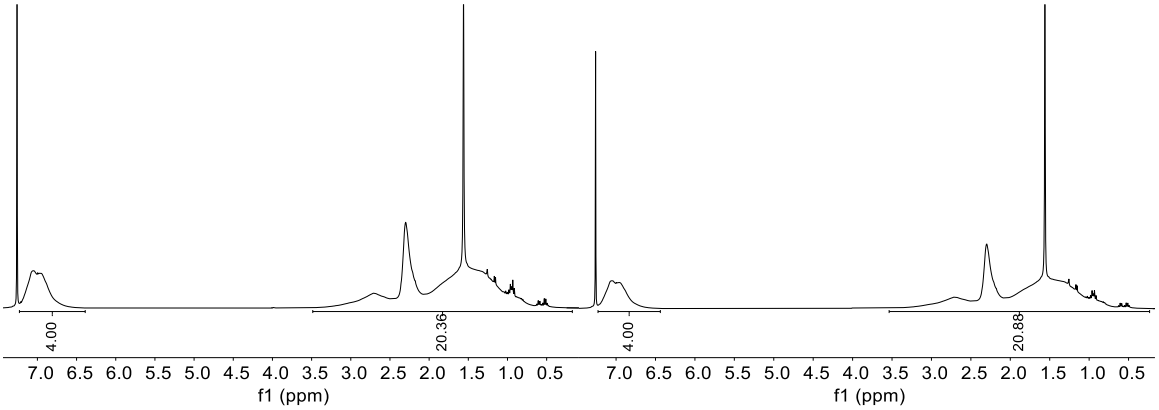

Fig. S18 ^{1}H NMR spectrum in $CDCl_3$ of poly(ethylene-co-toluene) product in Table S3, Entry 3a (left) and 3b (right)

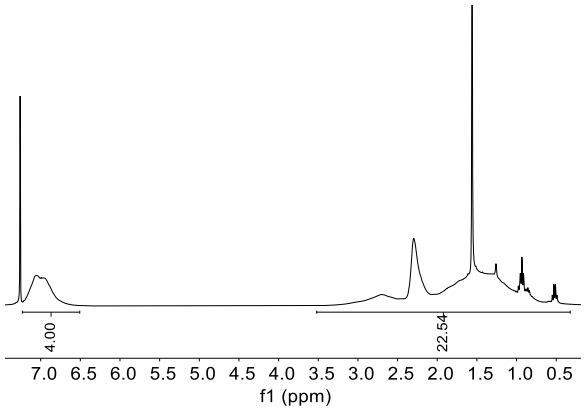

Fig. S19 ^{1}H NMR spectrum in $CDCl_3$ of poly(ethylene-co-toluene) product in Table S3, Entry 3c

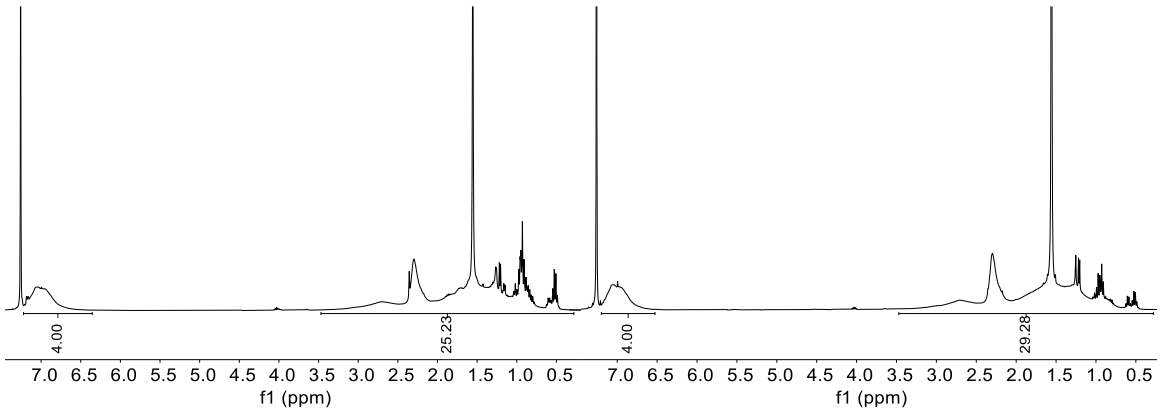

Fig. S20 ^{1}H NMR spectrum in $CDCl_3$ of poly(ethylene-co-toluene) product in Table S3, Entry 4a (left) and 4b (right)

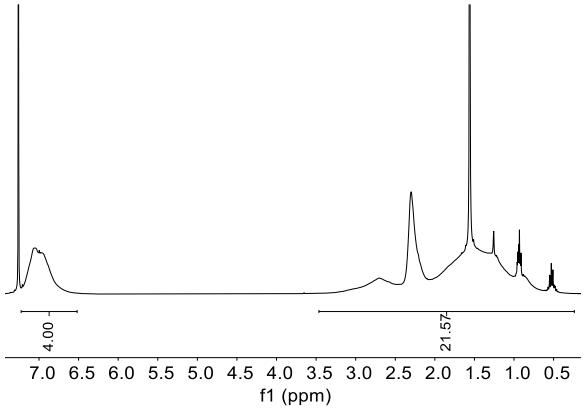

Fig. S21 ^{1}H NMR spectrum in $CDCl_3$ of poly(ethylene-co-toluene) product in Table S3, Entry 4c

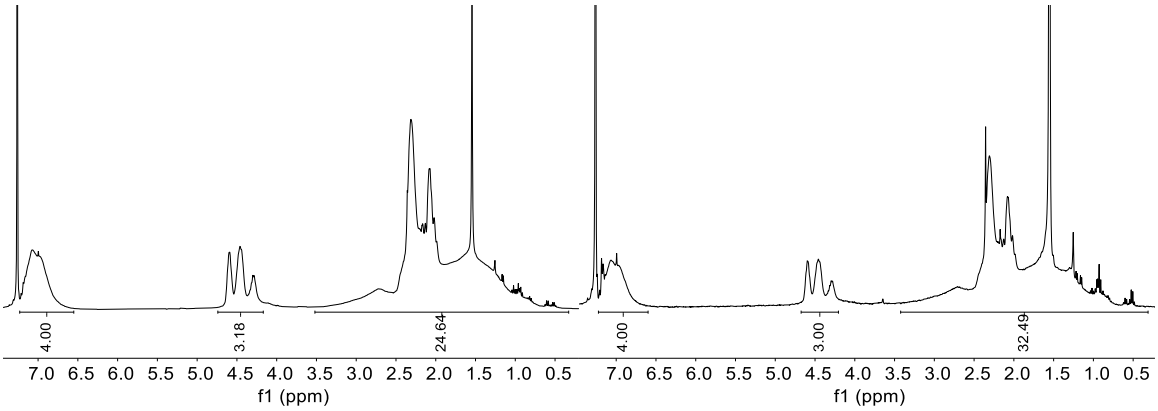

Fig. S22 ^{1}H NMR spectrum in $CDCl_3$ of poly(vinyl chloride-co-ethylene-co-toluene) product in Table S3, Entry 5a (left) and 5b (right)

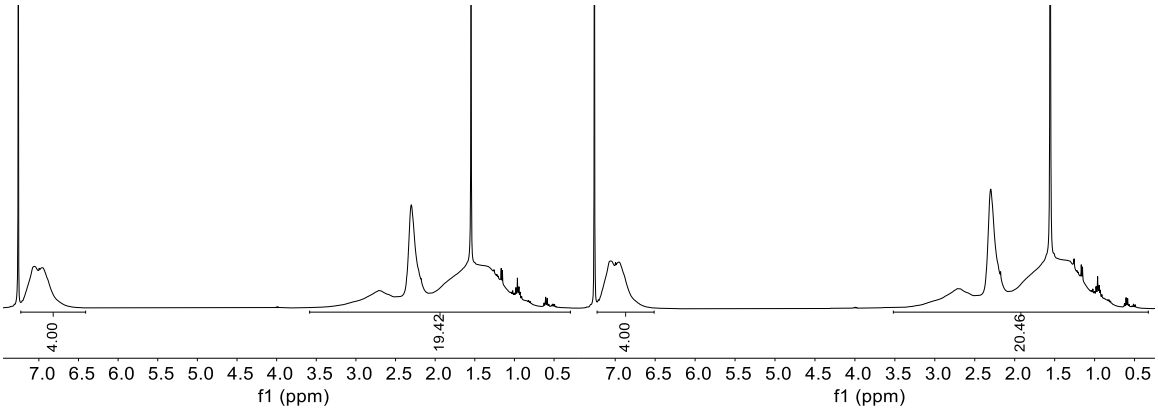

Fig. S23 ^{1}H NMR spectrum in $CDCl_3$ of poly(ethylene-co-toluene) product in Table S3, Entry 6a (left) and 6b (right)

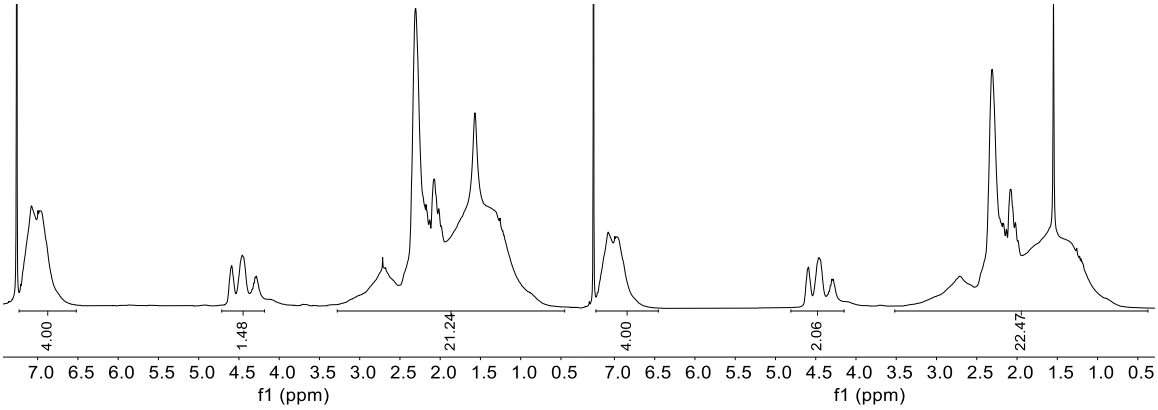

Fig. S24 ^{1}H NMR spectrum in $CDCl_3$ of poly(vinyl chloride-co-ethylene-co-toluene) product in Table S4, Entry 1a (left) and 1b (right)

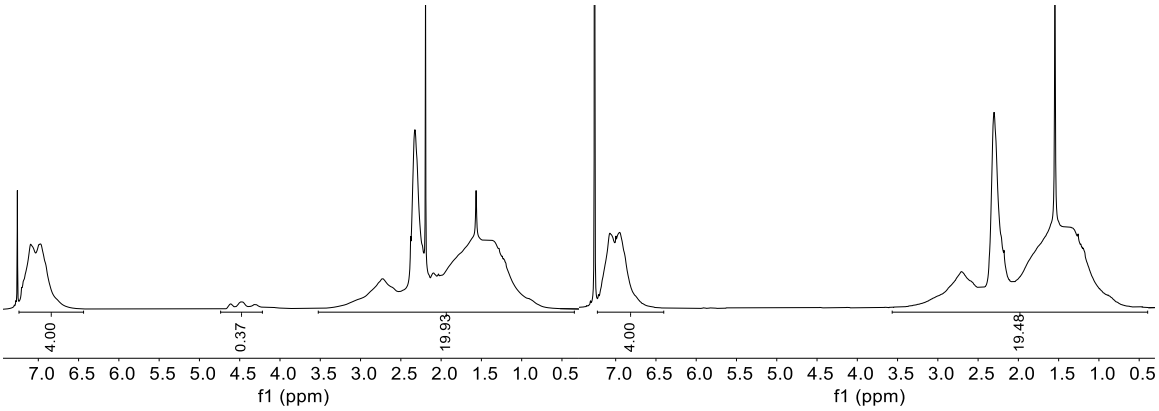

Fig. S25 ^{1}H NMR spectrum in $CDCl_3$ of poly(vinyl chloride-co-ethylene-co-toluene) product in Table S4, Entry 2a (left) and 2b (right)

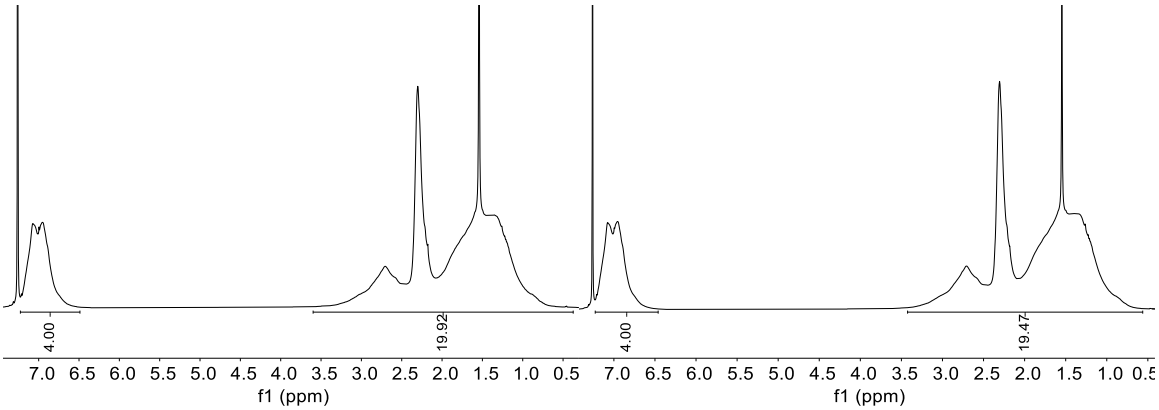

Fig. S26 ^{1}H NMR spectrum in $CDCl_3$ of poly(ethylene-co-toluene) product in Table S4, Entry 3a (left) and 3b (right)

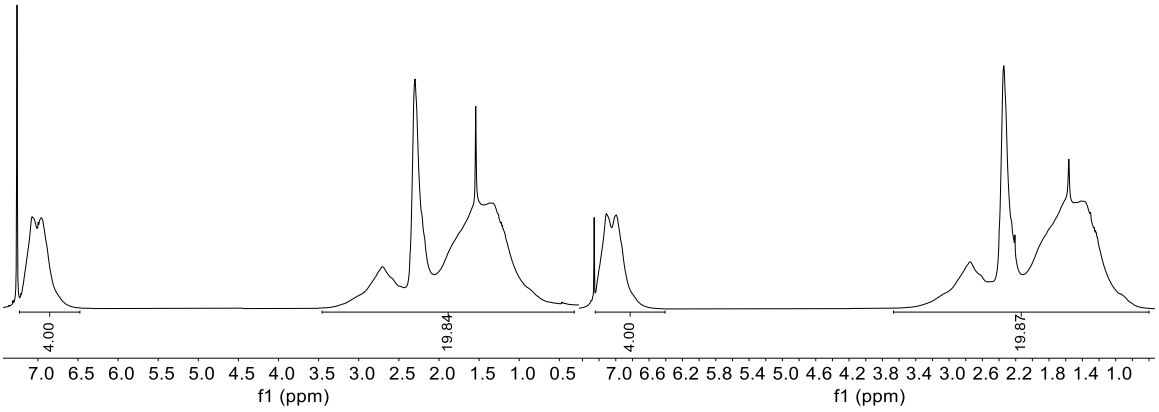

Fig. S27 ^{1}H NMR spectrum in $CDCl_3$ of poly(ethylene-co-toluene) product in Table S4, Entry 4a (left) and 4b (right)

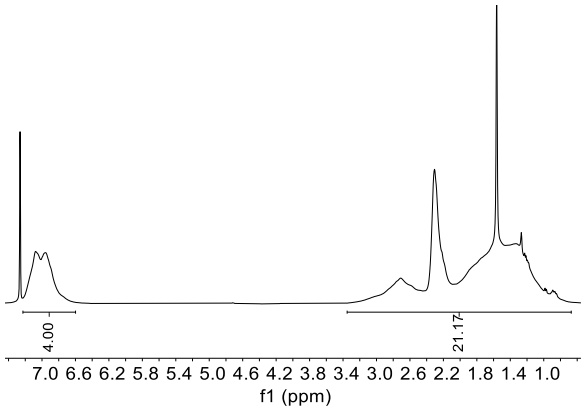

Fig. S28 ^{1}H NMR spectrum in $CDCl_3$ of poly(ethylene-co-toluene) product in Table S4, Entry 4c

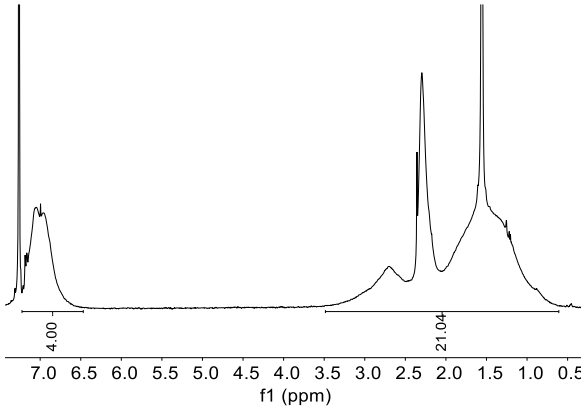

Fig. S29 ^{1}H NMR spectrum in $CDCl_3$ of poly(ethylene-co-toluene) product in Table S4, Entry 5

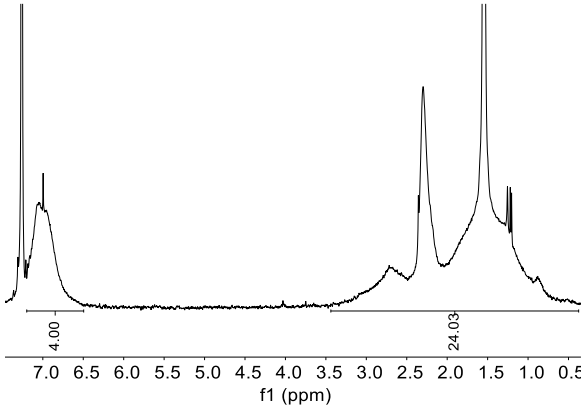

Fig. S30 ^{1}H NMR spectrum in $CDCl_3$ of poly(ethylene-co-toluene) product in Table S4, Entry 6

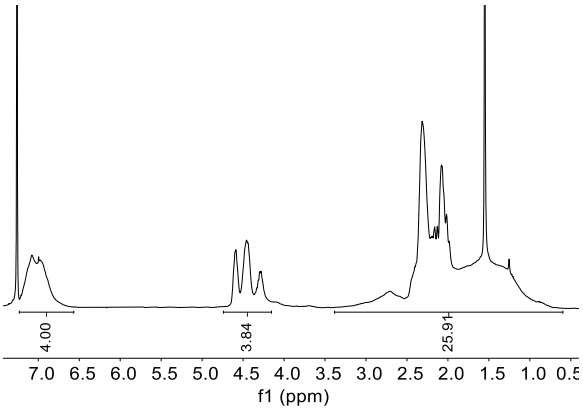

Fig. S31 ^{1}H NMR spectrum in $CDCl_3$ of poly(vinyl chloride-co-ethylene-co-toluene) product in Table S4, Entry 7 and Table 2, Entry 1

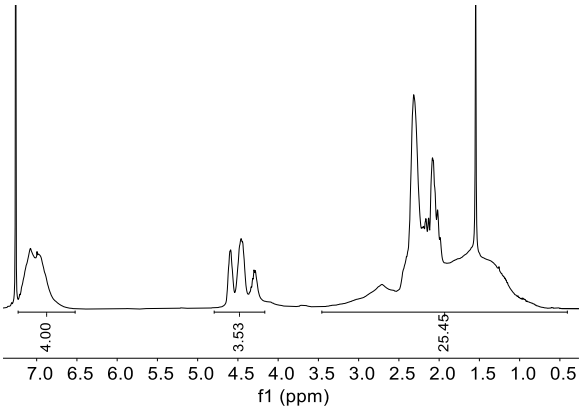

Fig. S32 ^{1}H NMR spectrum in $CDCl_3$ of poly(vinyl chloride-co-ethylene-co-toluene) product in Table S4, Entry 8 and Table 2, Entry 2

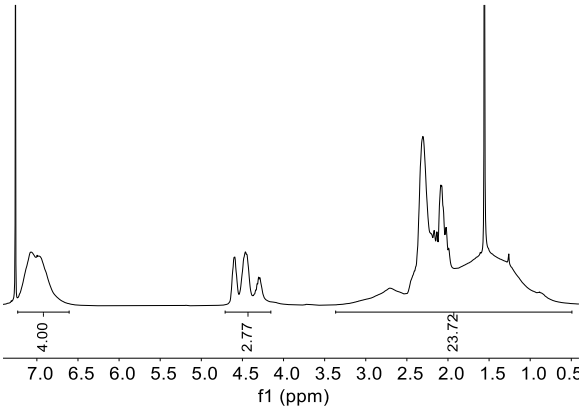

Fig. S33 ^{1}H NMR spectrum in $CDCl_3$ of poly(vinyl chloride-co-ethylene-co-toluene) product in Table S4, Entry 9 and Table 2, Entry 7

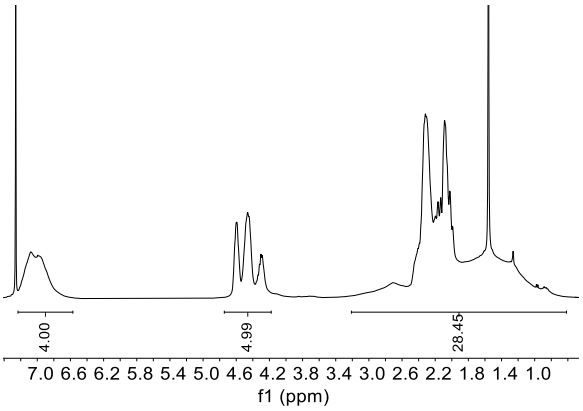

Fig. S34 ^{1}H NMR spectrum in $CDCl_3$ of poly(vinyl chloride-co-ethylene-co-toluene) product in Table S4, Entry 10 and Table 2, Entry 8

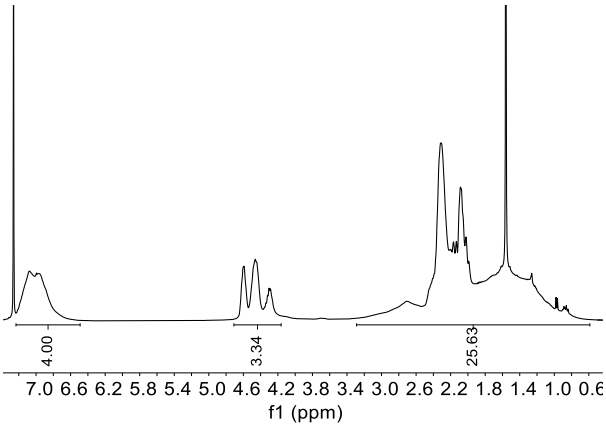

Fig. S35 ^{1}H NMR spectrum in $CDCl_3$ of poly(vinyl chloride-co-ethylene-co-toluene) product in Table S4, Entry 11 and Table 2, Entry 9

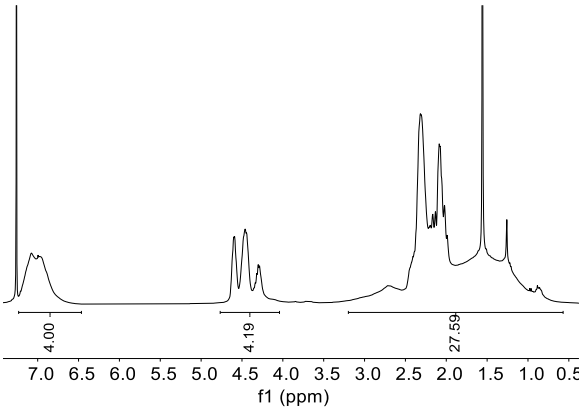

Fig. S36 ^{1}H NMR spectrum in $CDCl_3$ of poly(vinyl chloride-co-ethylene-co-toluene) product in Table S4, Entry 12 and Table 2, Entry 10

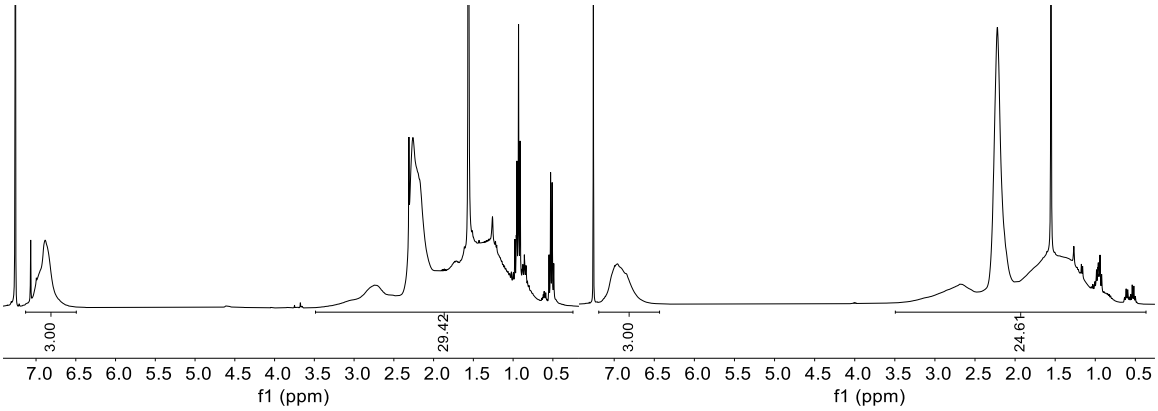

Fig. S37 ^{1}H NMR spectrum in $CDCl_3$ of poly(ethylene-co-o-xylene) product in Table S5, Entry 1a (left) and 1b (right)

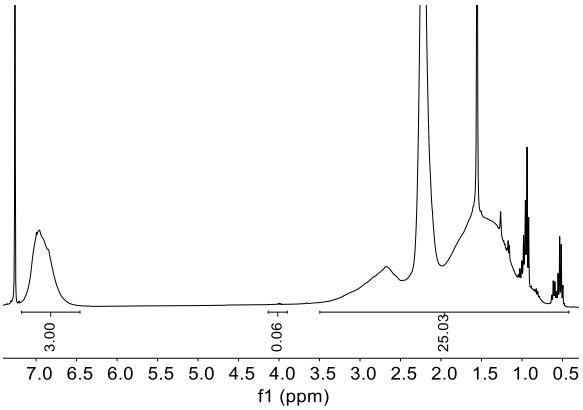

Fig. S38 ^{1}H NMR spectrum in $CDCl_3$ of poly(ethylene-co-o-xylene) product in Table S5, Entry 1c

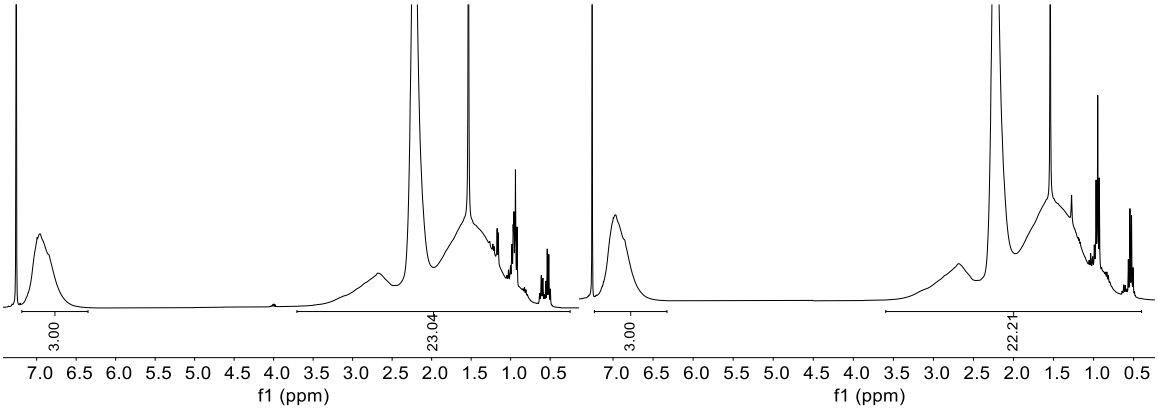

Fig. S39 ^{1}H NMR spectrum in $CDCl_3$ of poly(ethylene-co-o-xylene) product in Table S5, Entry 2a (left) and 2b (right)

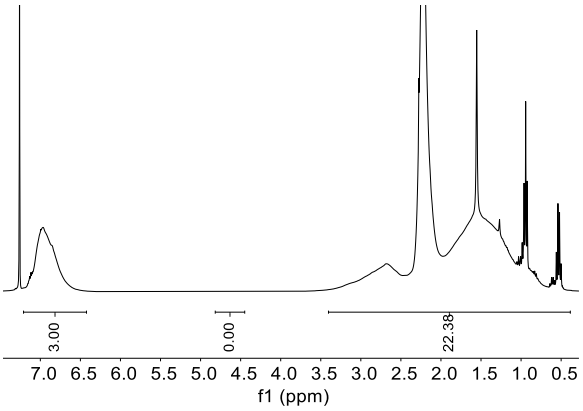

Fig. S40 ^{1}H NMR spectrum in $CDCl_3$ of poly(ethylene-co-o-xylene) product in Table S5, Entry 2c

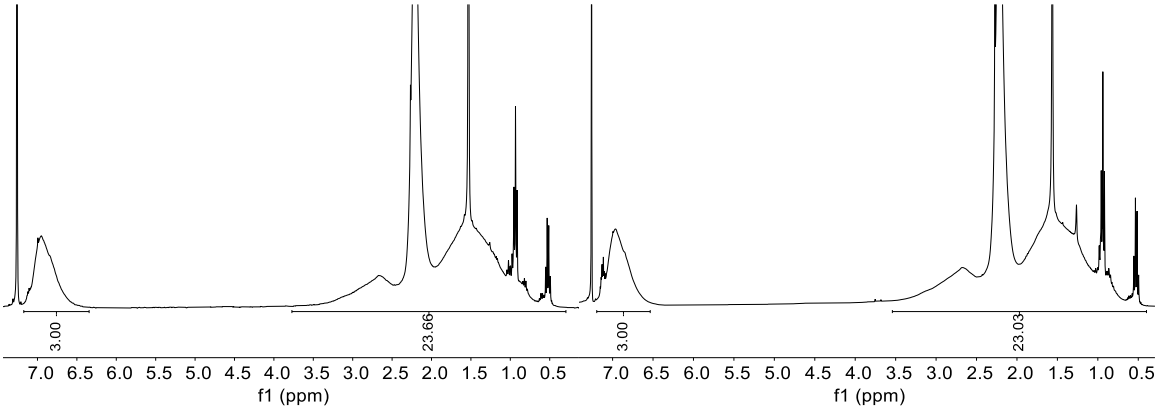

Fig. S41 ^{1}H NMR spectrum in $CDCl_3$ of poly(ethylene-co-o-xylene) product in Table S5, Entry 3a (left) and 3b (right)

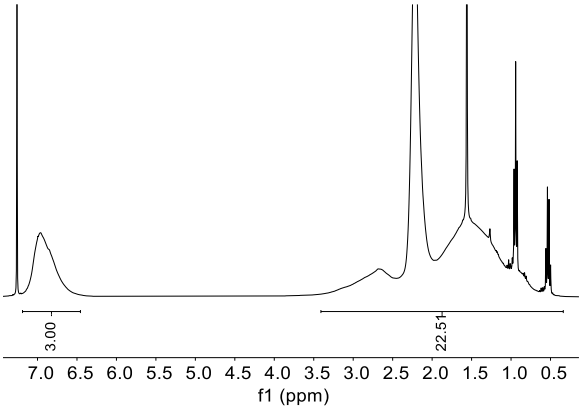

Fig. S42 ^{1}H NMR spectrum in $CDCl_3$ of poly(ethylene-co-o-xylene) product in Table S5, Entry 3c

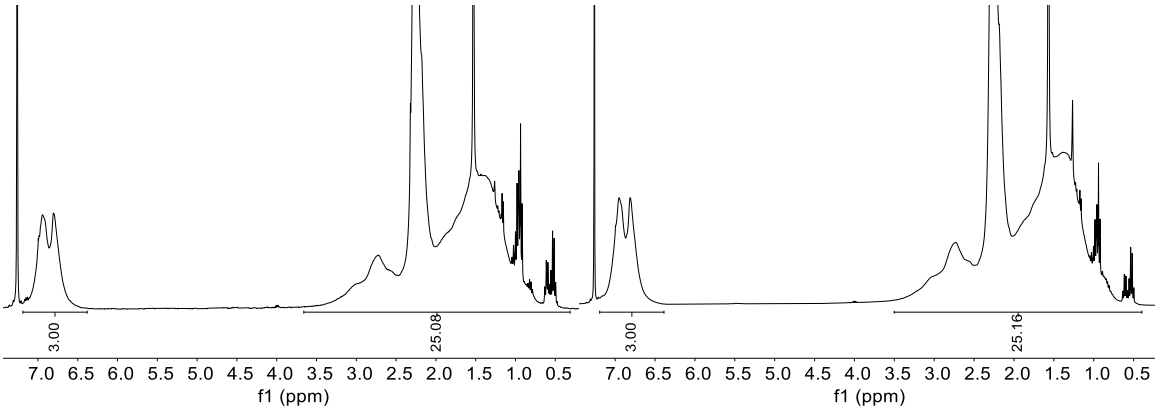

Fig. S43 ^{1}H NMR spectrum in $CDCl_3$ of poly(ethylene-co-m-xylene) product in Table S6, Entry 1a (left) and 1b (right)

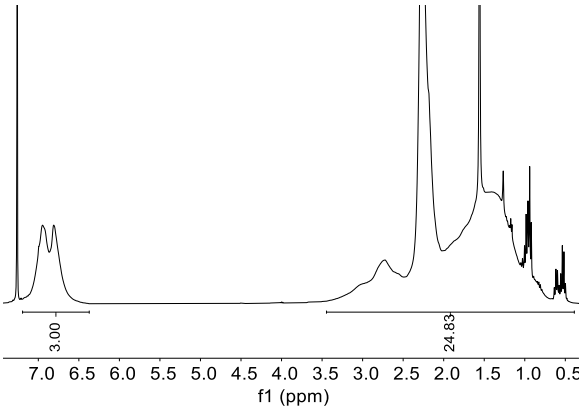

Fig. S44 ^{1}H NMR spectrum in $CDCl_3$ of poly(ethylene-co-m-xylene) product in Table S6, Entry 1c

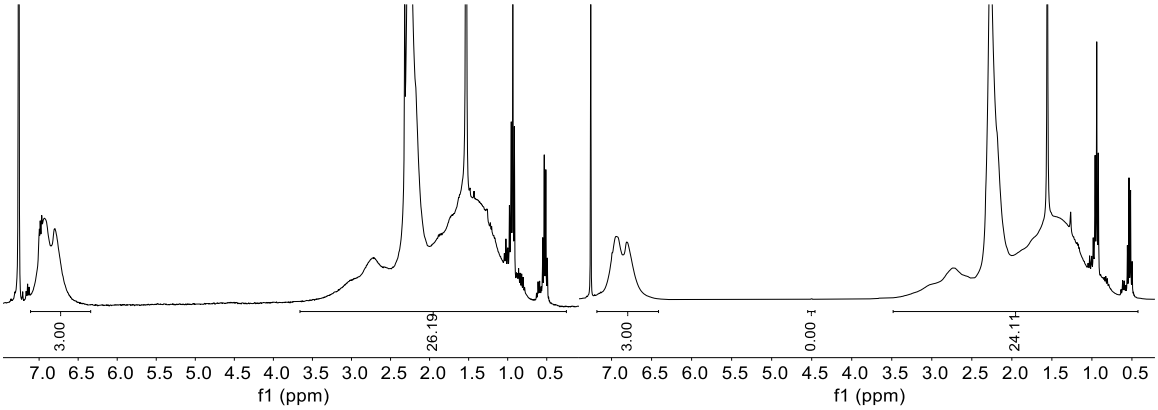

Fig. S45 ^{1}H NMR spectrum in $CDCl_3$ of poly(ethylene-co-m-xylene) product in Table S6, Entry 2a (left) and 2b (right)

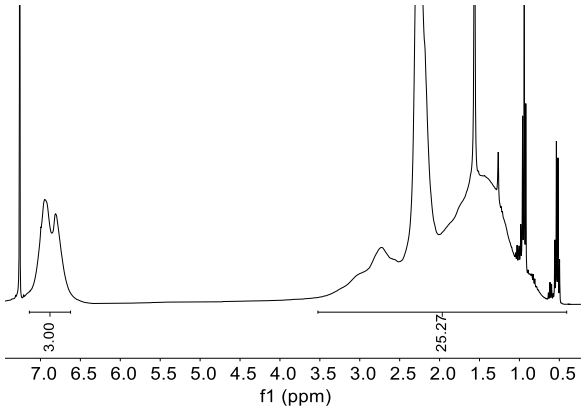

Fig. S46 ^{1}H NMR spectrum in $CDCl_3$ of poly(ethylene-co-m-xylene) product in Table S6, Entry 2c

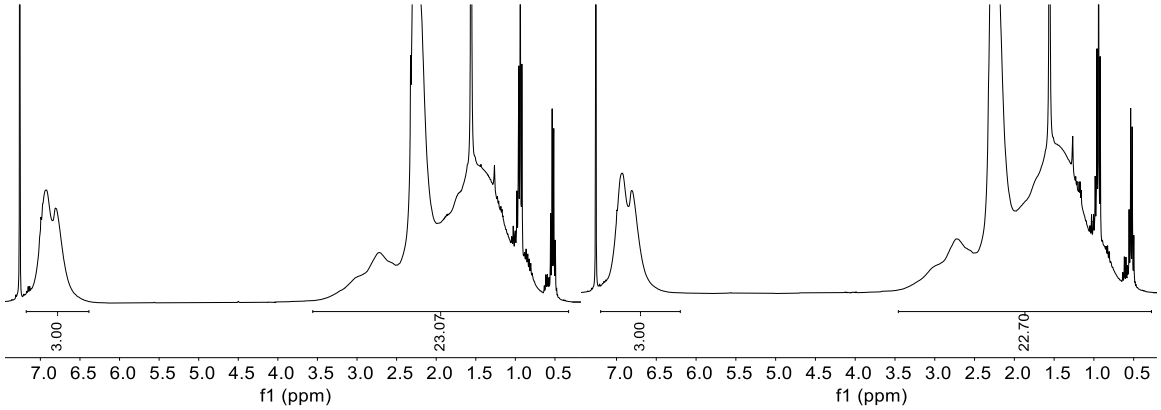

Fig. S47 ^{1}H NMR spectrum in $CDCl_3$ of poly(ethylene-co-m-xylene) product in Table S6, Entry 3a (left) and 3b (right)

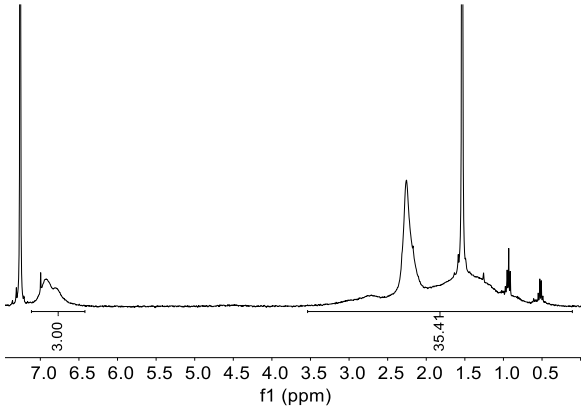

Fig. S48 ^{1}H NMR spectrum in $CDCl_3$ of poly(ethylene-co-m-xylene) product in Table S6, Entry 3c

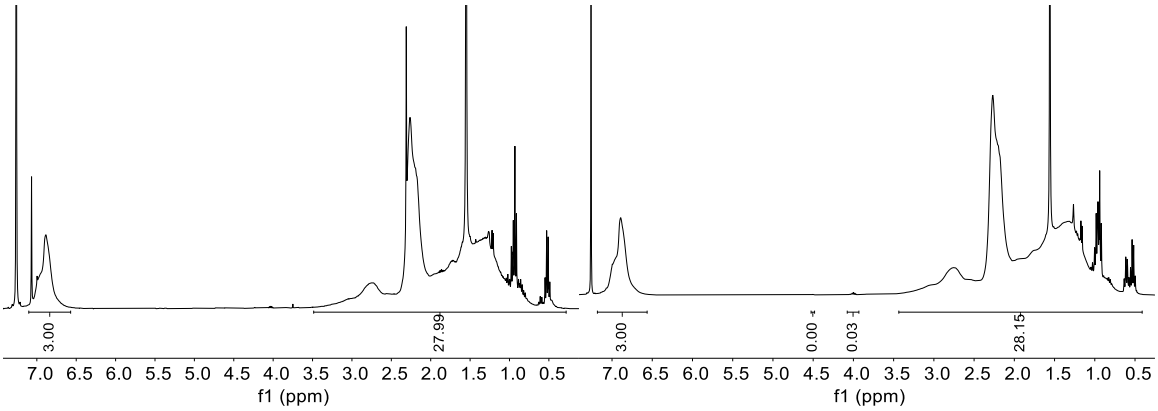

Fig. S49 ^{1}H NMR spectrum in $CDCl_3$ of poly(ethylene-co-p-xylene) product in Table S7, Entry 1a (left) and 1b (right)

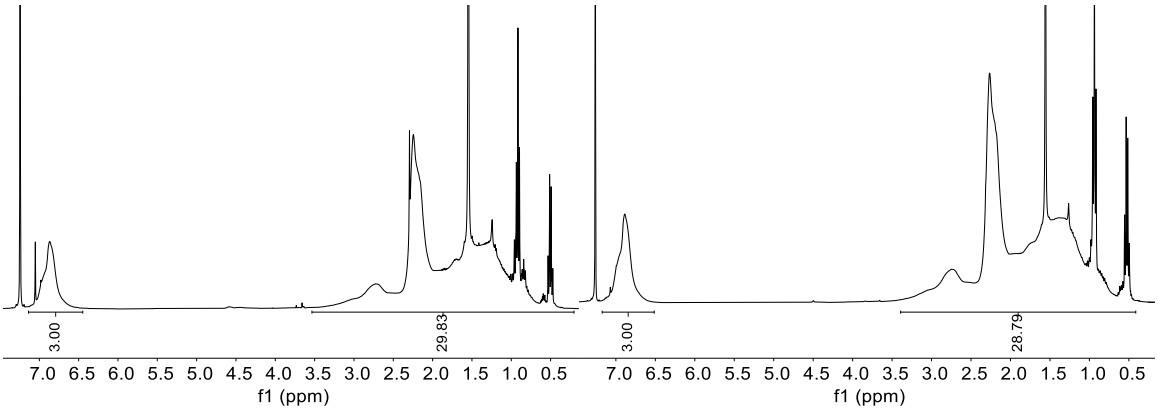

Fig. S50 ^{1}H NMR spectrum in $CDCl_3$ of poly(ethylene-co-p-xylene) product in Table S7, Entry 2a (left) and 2b (right)

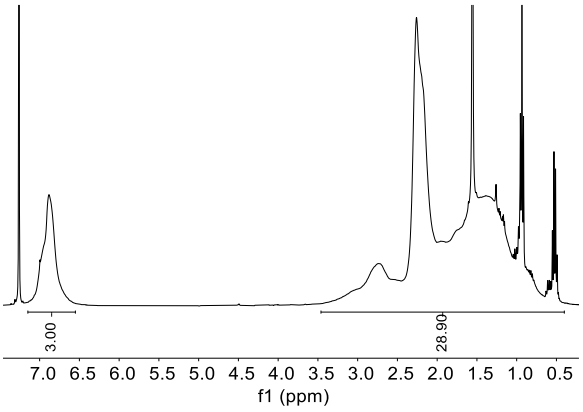

Fig. S51 ^{1}H NMR spectrum in $CDCl_3$ of poly(ethylene-co-p-xylene) product in Table S7, Entry 2c

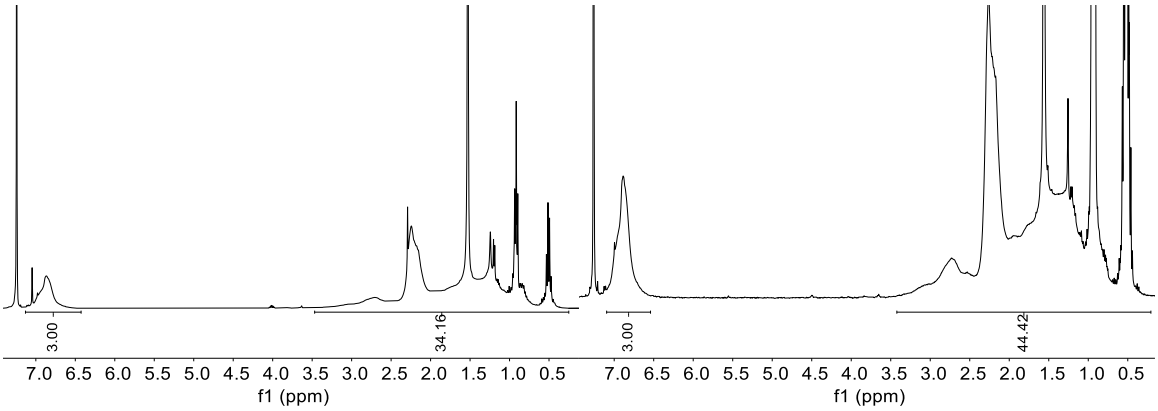

Fig. S52 ^{1}H NMR spectrum in $CDCl_3$ of poly(ethylene-co-p-xylene) product in Table S7, Entry 3a (left) and 3b (right)

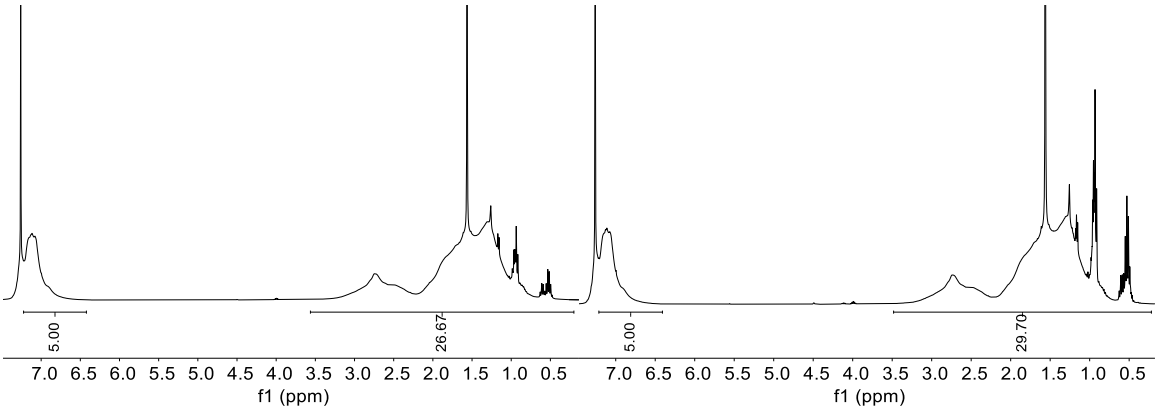

Fig. S53 ^{1}H NMR spectrum in $CDCl_3$ of poly(ethylene-co-benzene) product in Table S8, Entry 1a (left) and 1b (right)

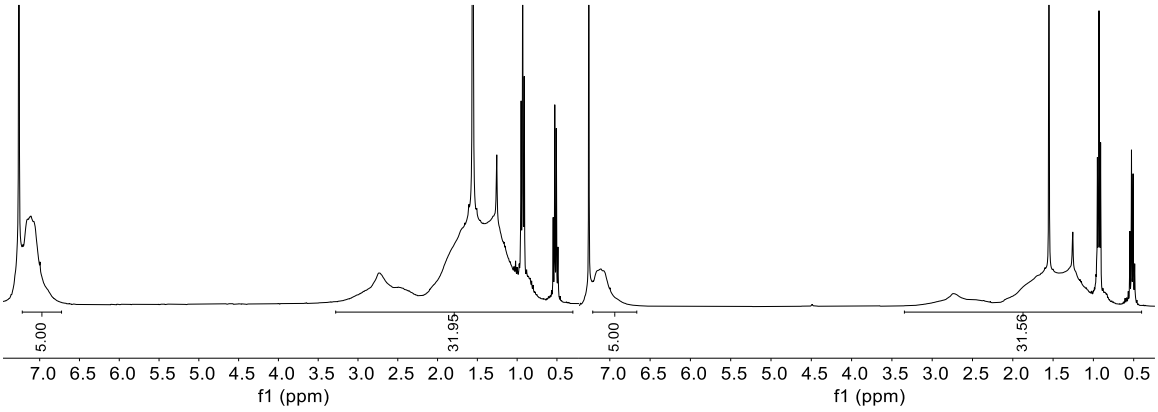

Fig. S54 ^{1}H NMR spectrum in $CDCl_3$ of poly(ethylene-co-benzene) product in Table S8, Entry 2a (left) and 2b (right)

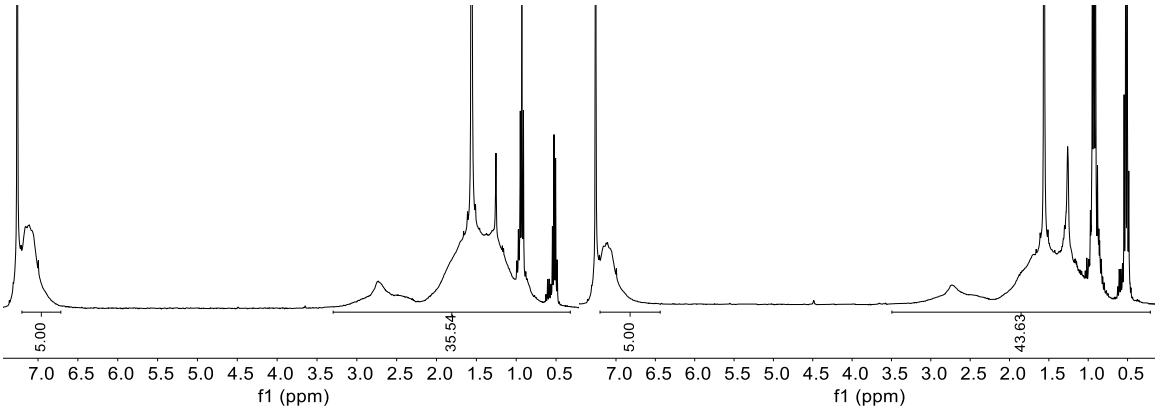

Fig. S55 ^{1}H NMR spectrum in $CDCl_3$ of poly(ethylene-co-benzene) product in Table S8, Entry 3a (left) and 3b (right)

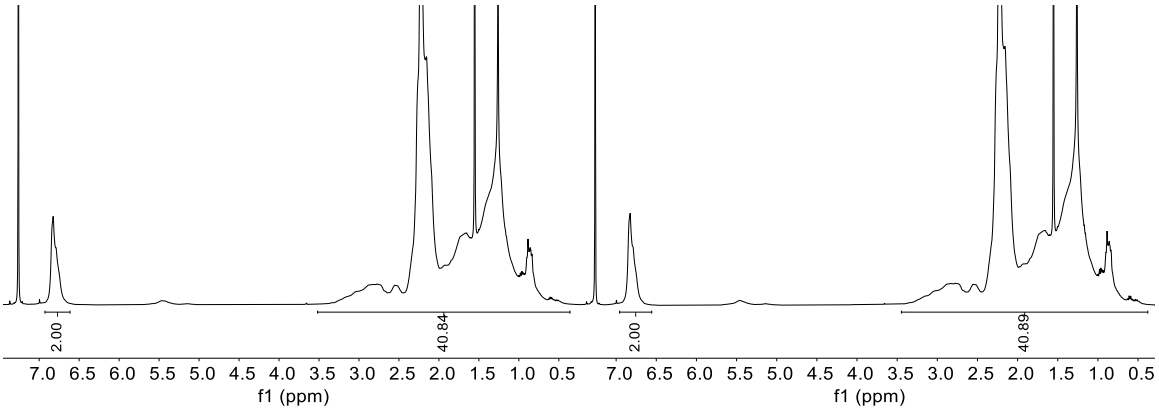

Fig. S56 ^{1}H NMR spectrum in $CDCl_3$ of poly(ethylene-co-mesitylene) product in Table S9, Entry 1a (left) and 1b (right)

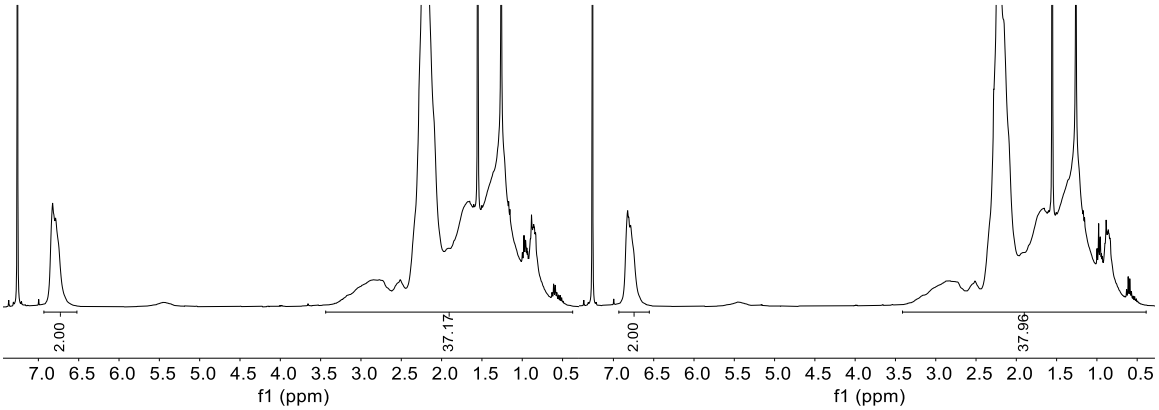

Fig. S57 ^{1}H NMR spectrum in $CDCl_3$ of poly(ethylene-co-mesitylene) product in Table S9, Entry 2a (left) and 2b (right)

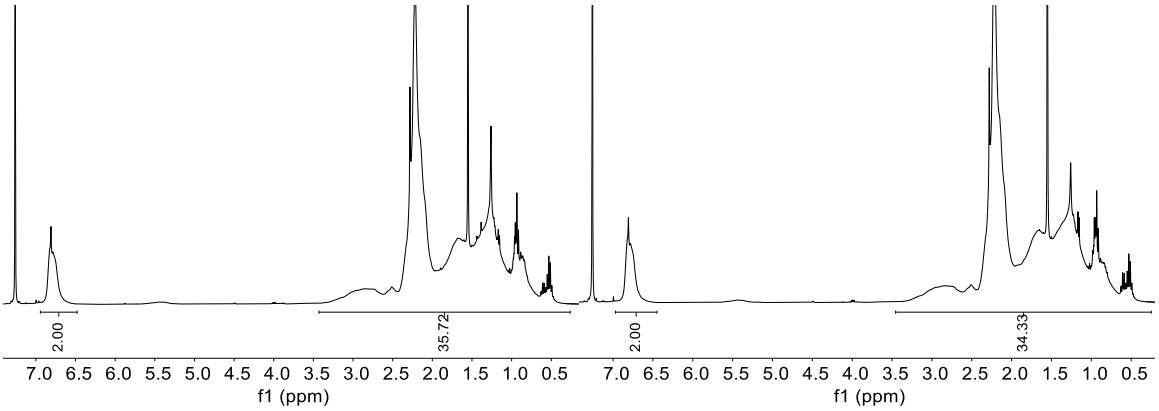

Fig. S58 ^{1}H NMR spectrum in $CDCl_3$ of poly(ethylene-co-mesitylene) product in Table S9, Entry 3a (left) and 3b (right)

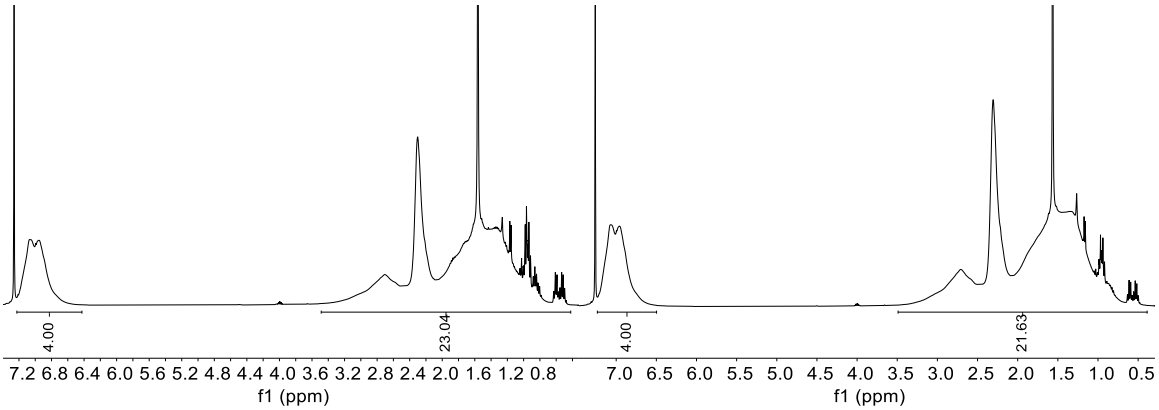

Fig. S59 ^{1}H NMR spectrum in $CDCl_3$ of poly(ethylene-co-toluene) product in Table S10, Entry 1a (left) and 1b (right)

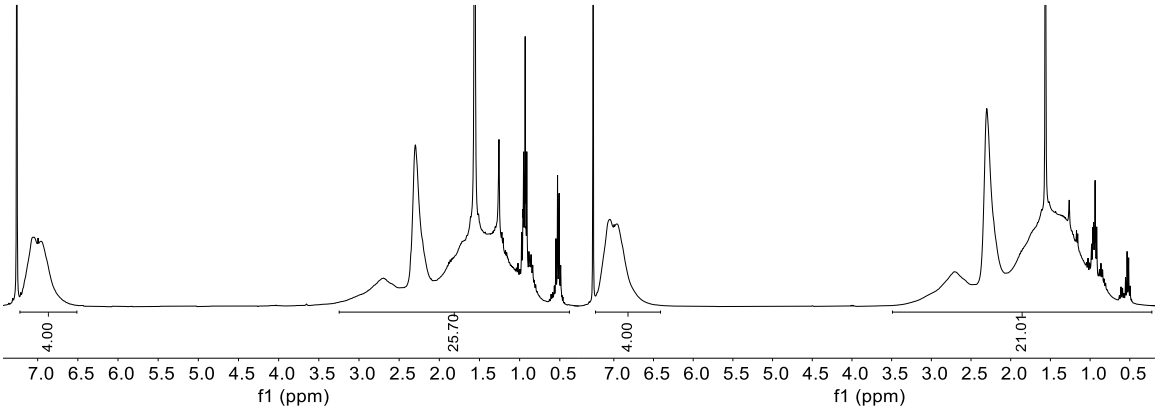

Fig. S60 ^{1}H NMR spectrum in $CDCl_3$ of poly(ethylene-co-toluene) product in Table S10, Entry 2a (left) and 2b (right)

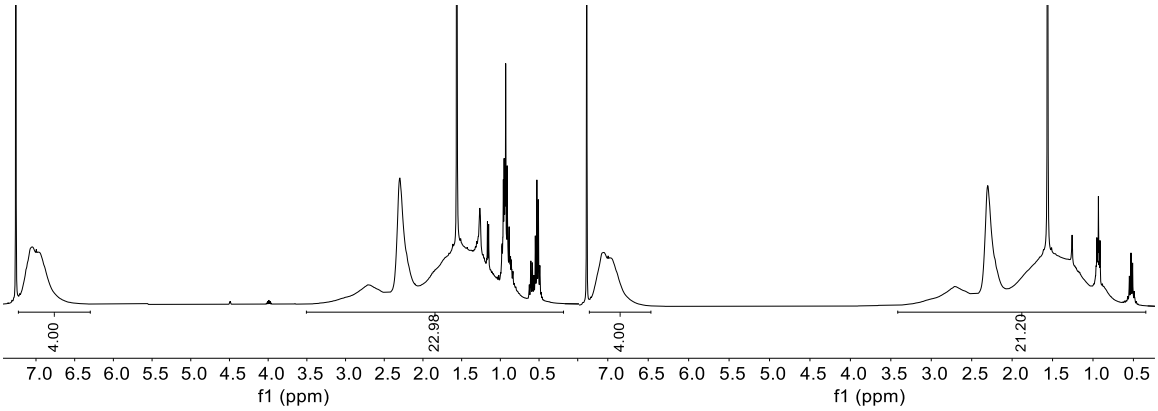

Fig. S61 ^{1}H NMR spectrum in $CDCl_3$ of poly(ethylene-co-toluene) product in Table S10, Entry 3a (left) and 3b (right)

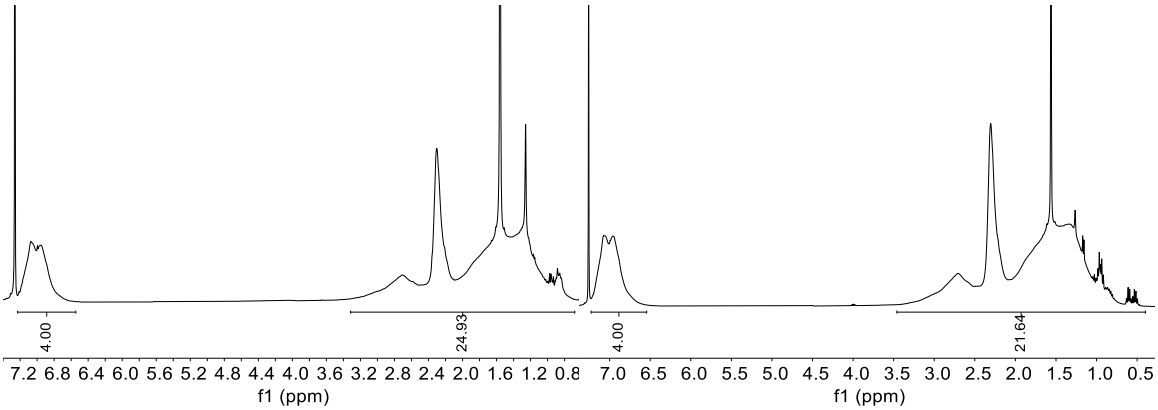

Fig. S62 ^{1}H NMR spectrum in $CDCl_3$ of poly(ethylene-co-toluene) product in Table S10, Entry 4a (left) and 4b (right)

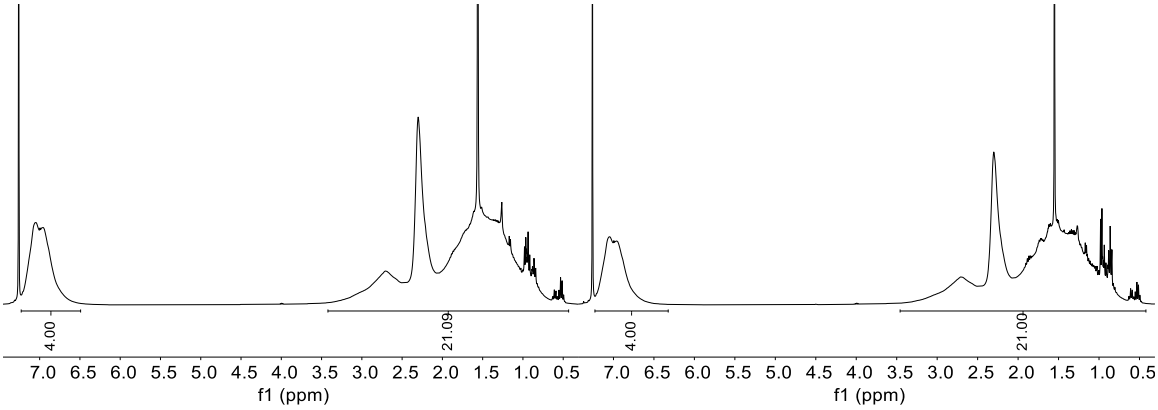

Fig. S63 ^{1}H NMR spectrum in $CDCl_3$ of poly(ethylene-co-toluene) product in Table S10, Entry 5a (left) and 5b (right)

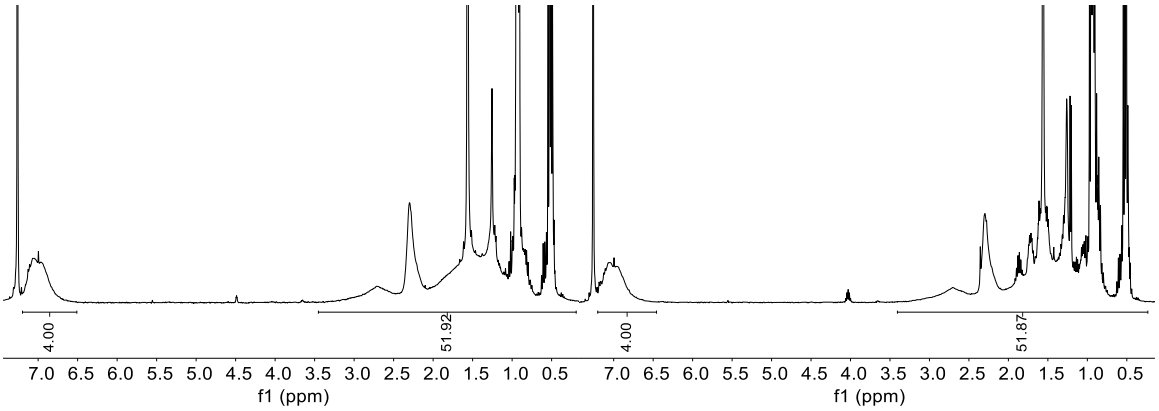

Fig. S64 ^{1}H NMR spectrum in $CDCl_3$ of poly(ethylene-co-toluene) product in Table S10, Entry 6a (left) and 6b (right)

5. FT-IR Spectroscopy

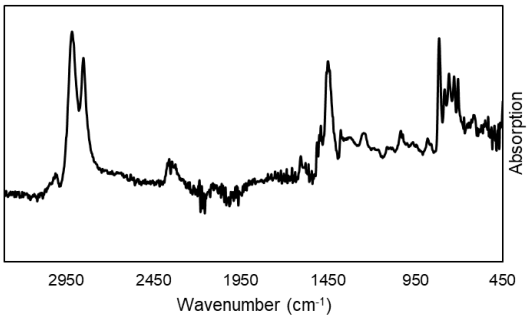

Fig. S65 FT-IR spectrum of Table S1, Entry 1

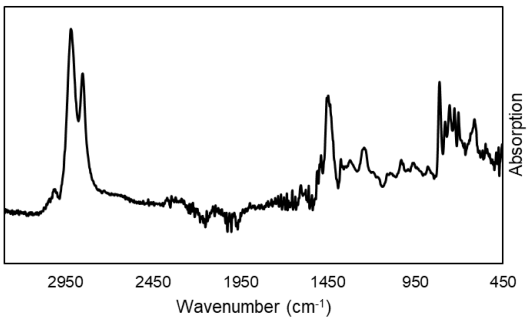

Fig. S66 FT-IR spectrum of Table S1, Entry 2

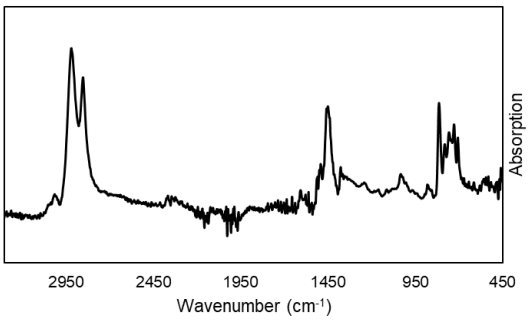

Fig. S67 FT-IR spectrum of Table S1, Entry 3

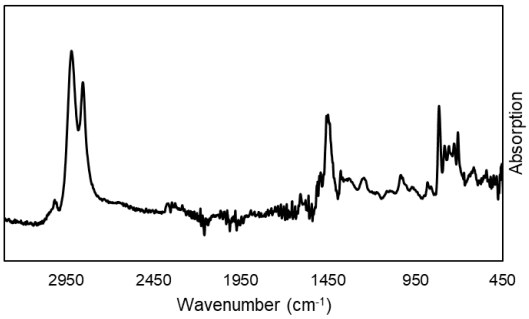

Fig. S68 FT-IR spectrum of Table S1, Entry 4

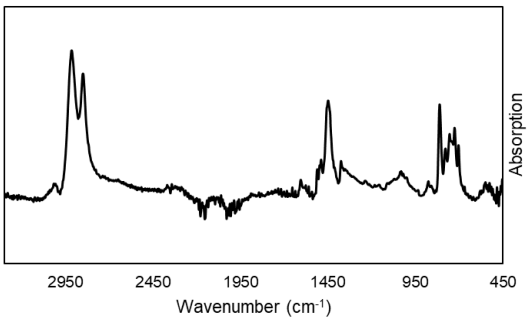

Fig. S69 FT-IR spectrum of Table S1, Entry 7

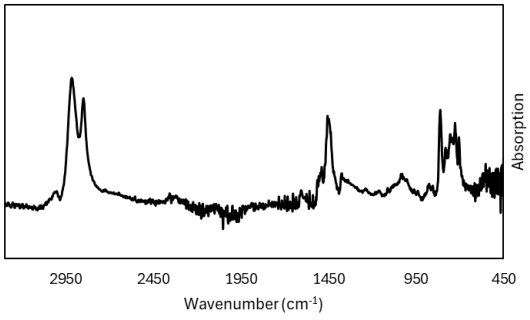

Fig. S70 FT-IR spectrum of Table S2, Entry 1

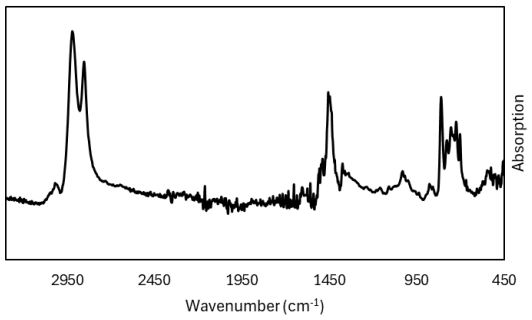

Fig. S71 FT-IR spectrum of Table S2, Entry 2

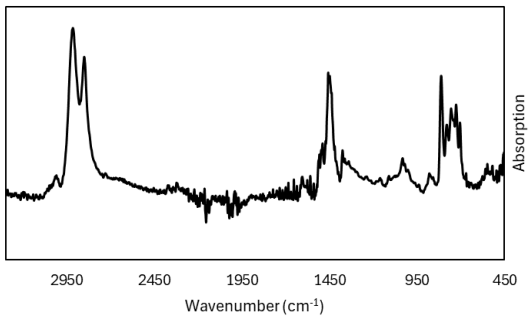

Fig. S72 FT-IR spectrum of Table S2, Entry 3

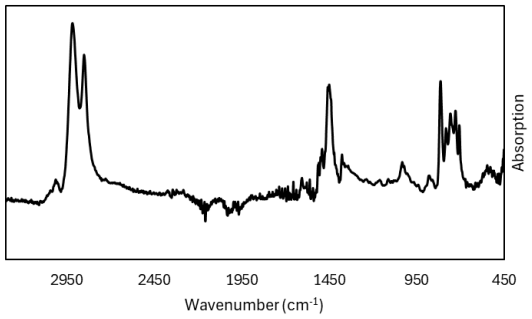

Fig. S73 FT-IR spectrum of Table S2, Entry 4

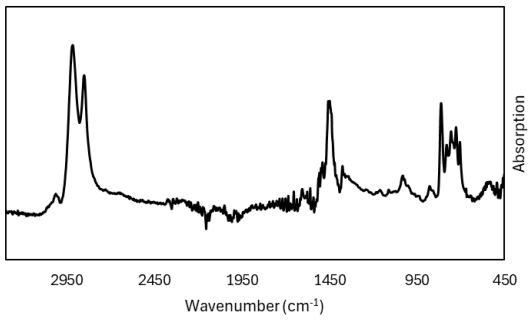

Fig. S74 FT-IR spectrum of Table S2, Entry 5

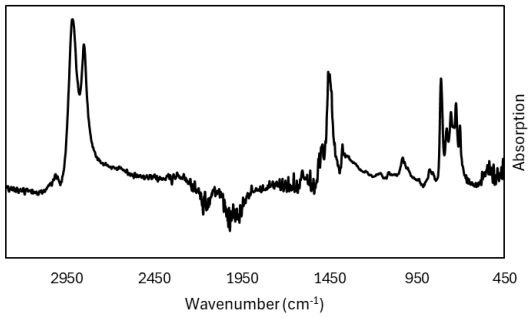

Fig. S75 FT-IR spectrum of Table S2, Entry 6

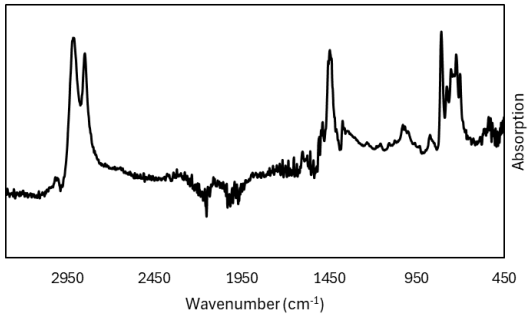

Fig. S76 FT-IR spectrum of Table S3, Entry 1b

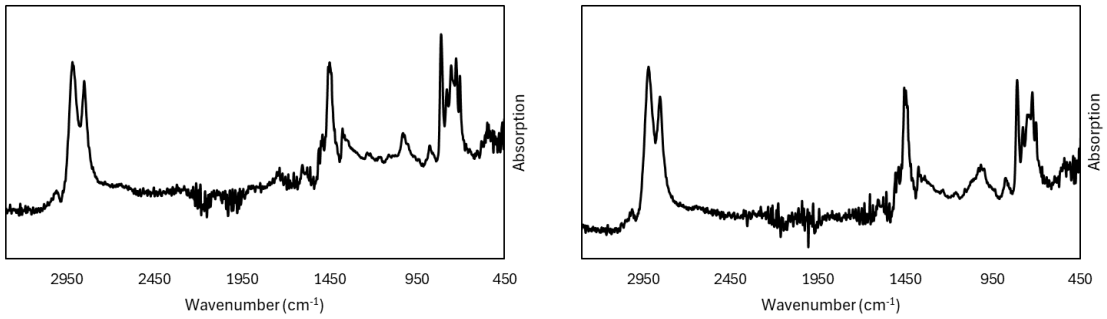

Fig. S77 FT-IR spectrum of Table S3, Entry 2a (left) and 2c (right)

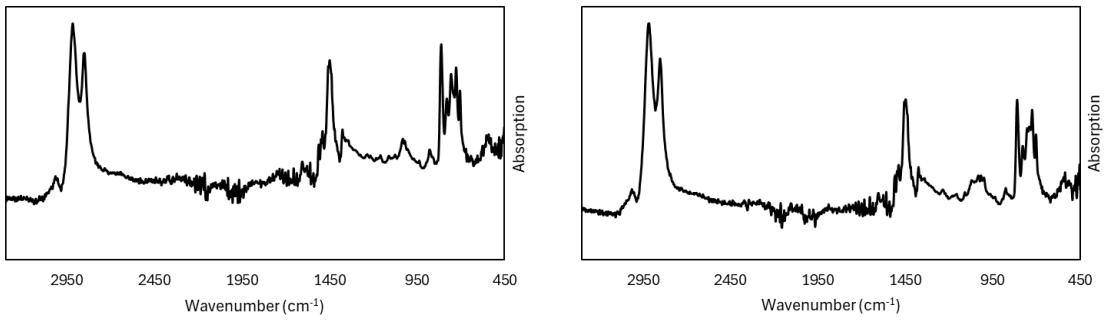

Fig. S78 FT-IR spectrum of Table S3, Entry 3a (left) and 3c (right)

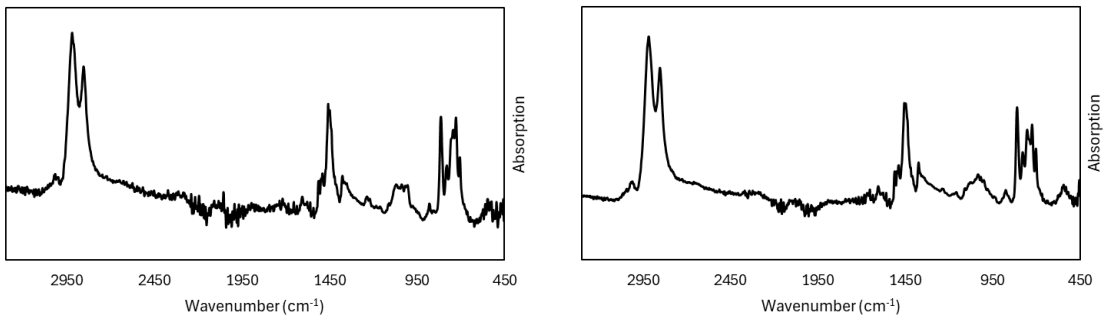

Fig. S79 FT-IR spectrum of Table S3, Entry 4a (left) and 4c (right)

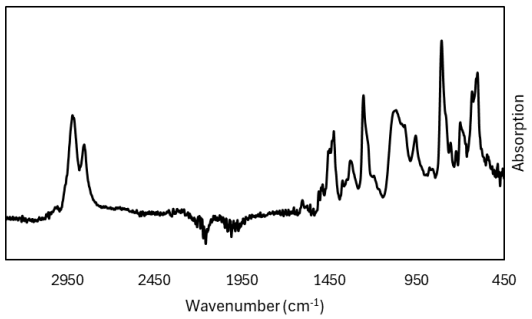

Fig. S80 FT-IR spectrum of Table 2, Entry 9

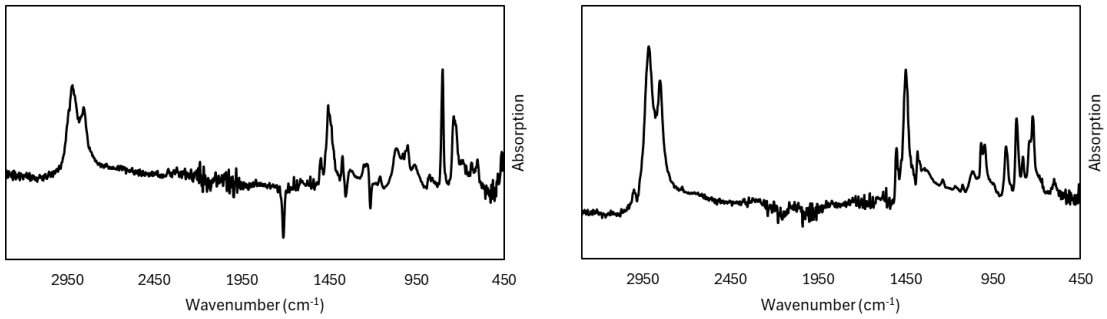

Fig. S81 FT-IR spectrum of Table S5, Entry 1b (left) and 1c (right)

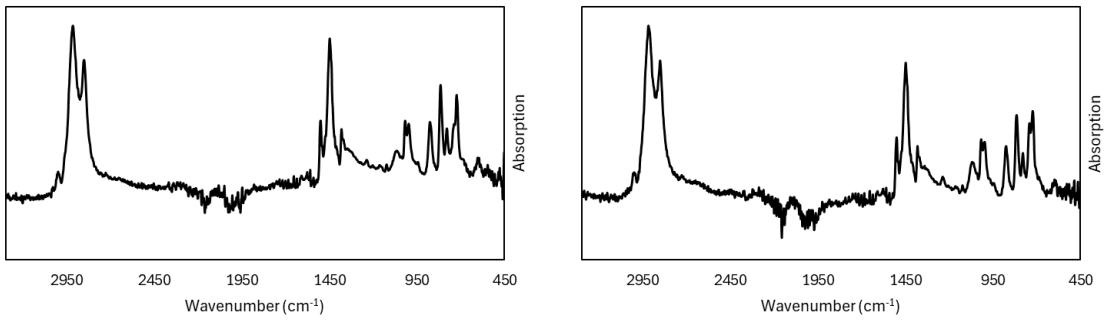

Fig. S82 FT-IR spectrum of Table S5, Entry 2b (left) and 2c (right)

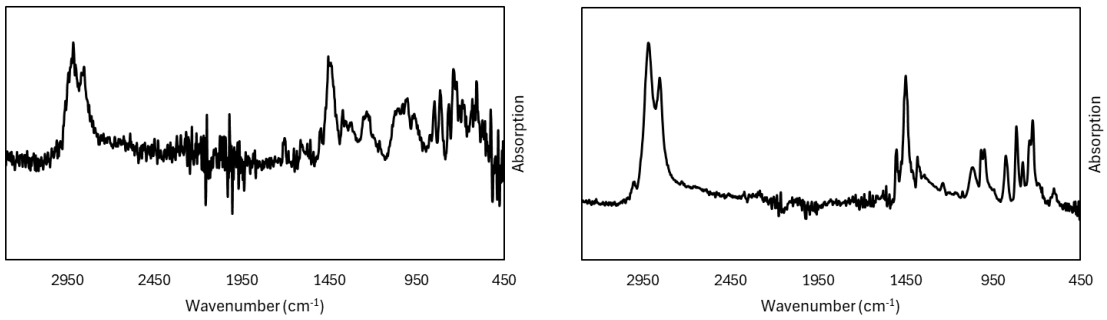

Fig. S83 FT-IR spectrum of Table S5, Entry 3b (left) and 3c (right)

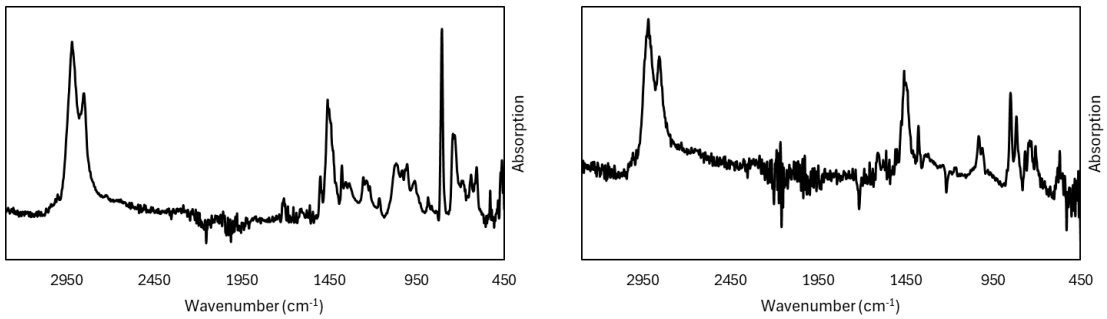

Fig. S84 FT-IR spectrum of Table S6, Entry 1b (left) and 1c (right)

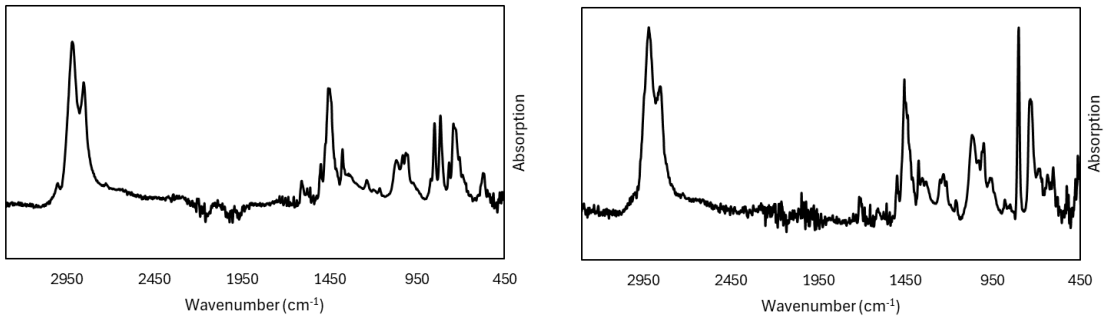

Fig. S85 FT-IR spectrum of Table S6, Entry 2b (left) and 2c (right)

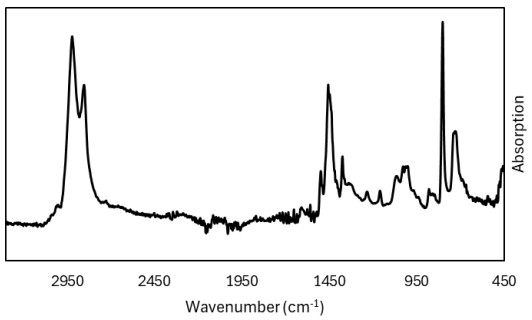

Fig. S86 FT-IR spectrum of Table S7, Entry 1b

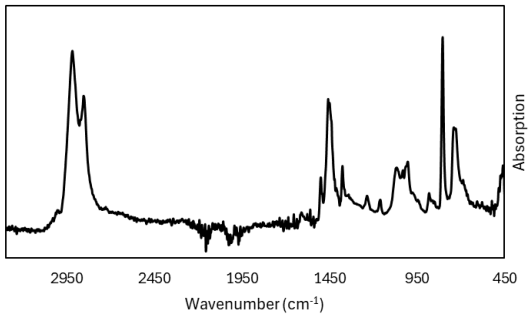

Fig. S87 FT-IR spectrum of Table S7, Entry 2b

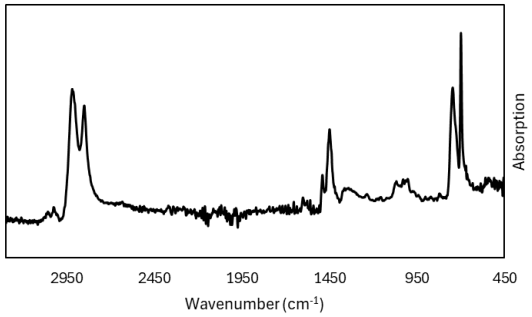

Fig. S88 FT-IR spectrum of Table S8, Entry 1b

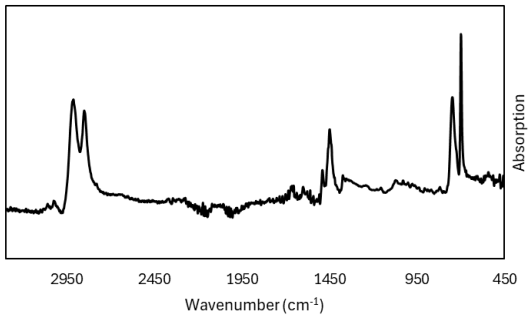

Fig. S89 FT-IR spectrum of Table S8, Entry 2a

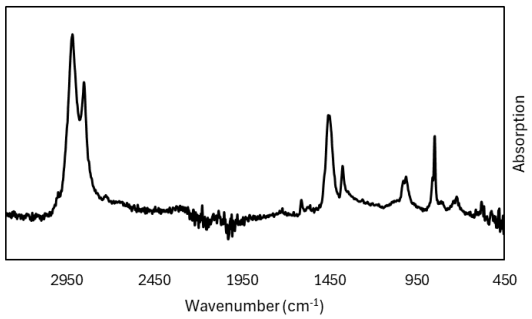

Fig. S90 FT-IR spectrum of Table S9, Entry 1a

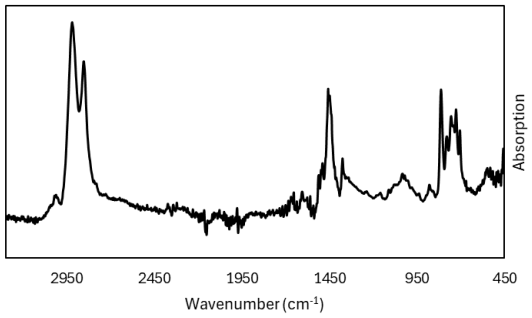

Fig. S91 FT-IR spectrum of Table S10, Entry 2b

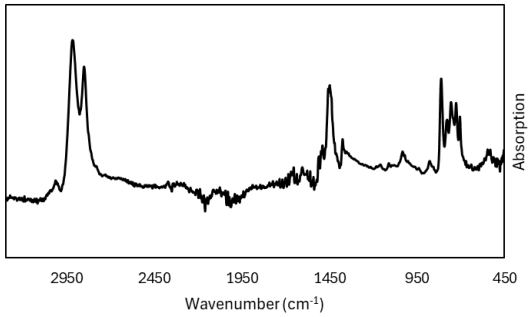

Fig. S92 FT-IR spectrum of Table S10, Entry 5a

6. Differential Scanning Calorimetry (DSC)

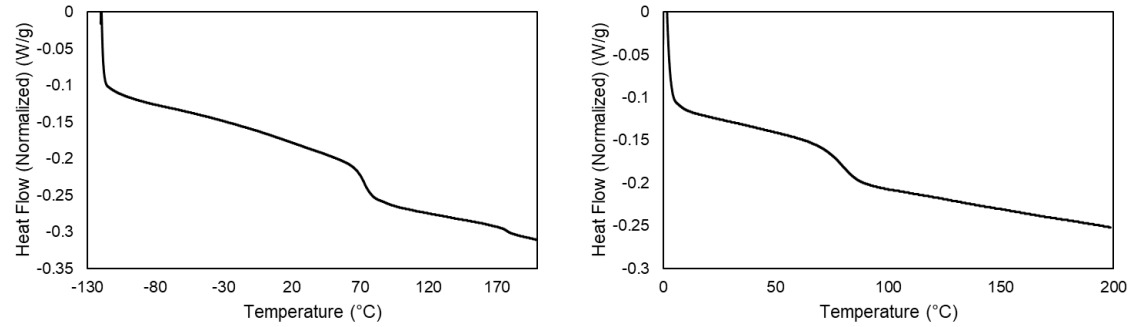

Fig. S93 DSC (2nd heating curve) of Table S3, Entry 1a (left) and 1b (right)

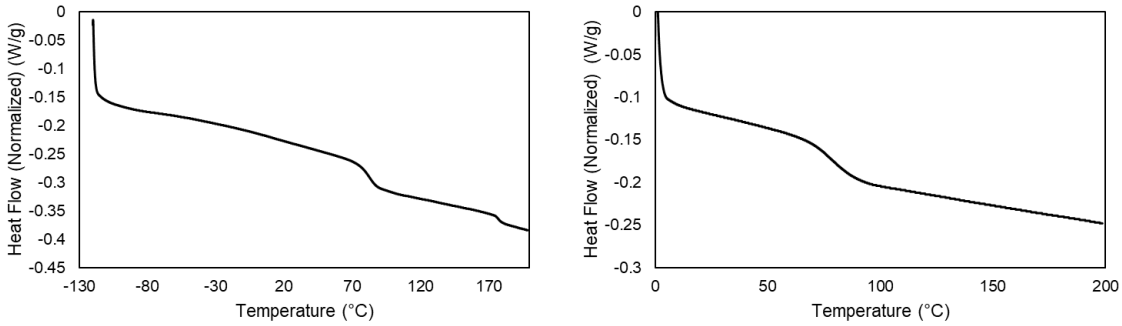

Fig. S94 DSC (2nd heating curve) of Table S3, Entry 2a (left) and 2c (right)

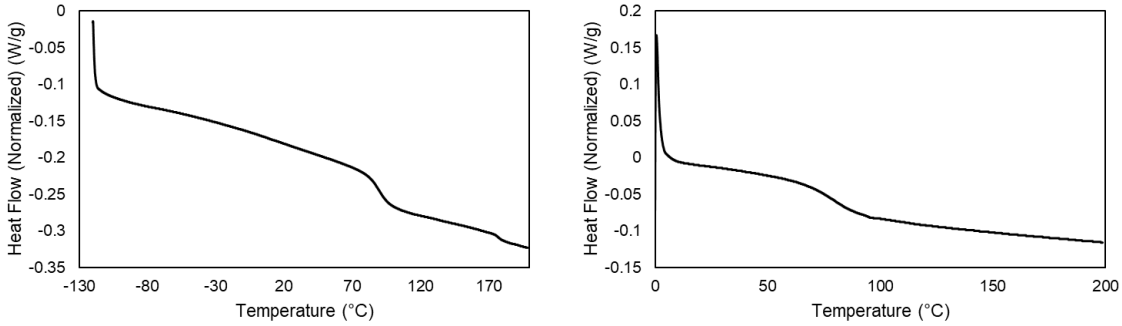

Fig. S95 DSC (2nd heating curve) of Table S3, Entry 3a (left) and 3c (right)

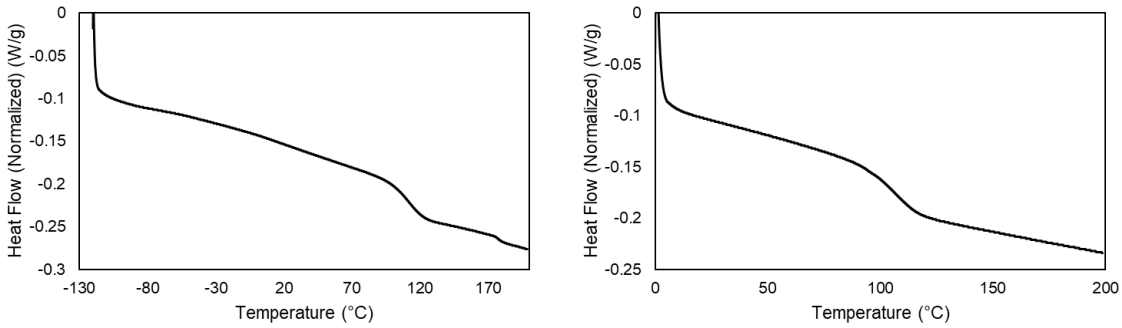

Fig. S96 DSC (2nd heating curve) of Table S3, Entry 4a (left) and 4c (right)

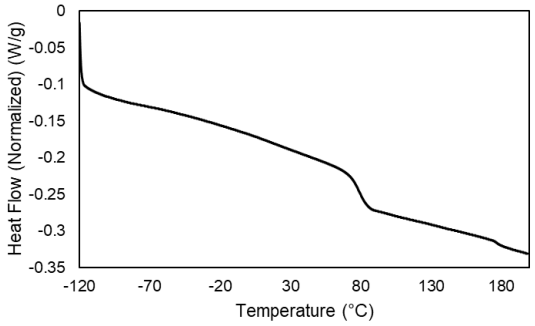

Fig. S97 DSC (2nd heating curve) of Table S3, Entry 6a

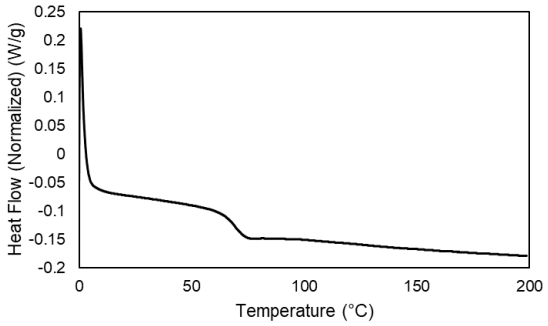

Fig. S98 DSC (2nd heating curve) of Table S4, Entry 2b

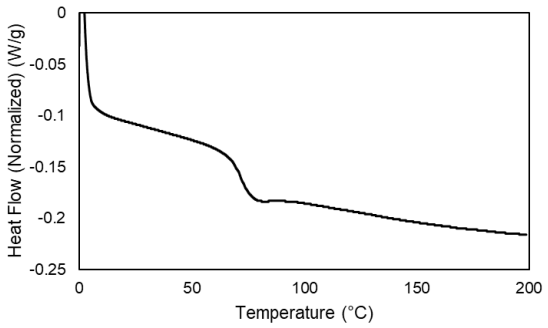

Fig. S99 DSC (2nd heating curve) of Table S4, Entry 4a

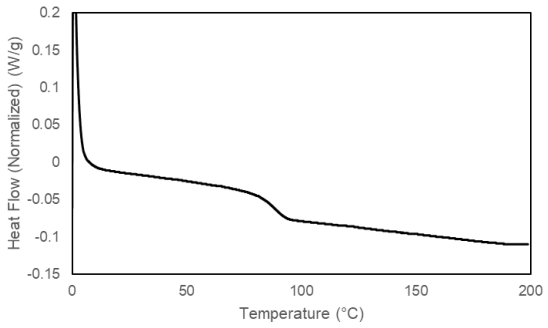

Fig. S100 DSC (2nd heating curve) of Table S4, Entry 5

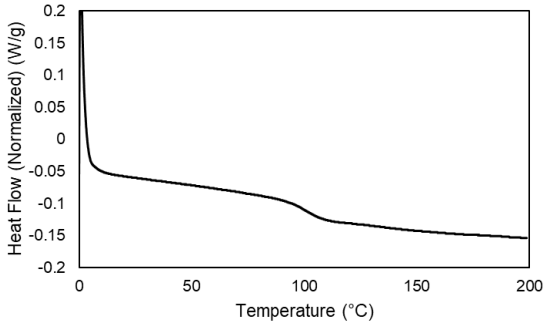

Fig. S101 DSC (2nd heating curve) of Table S4, Entry 6

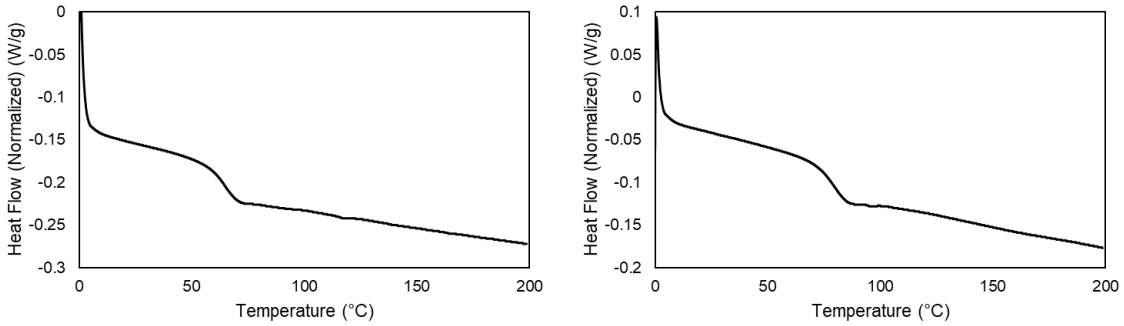

Fig. S102 DSC (2nd heating curve) of Table S5, Entry 1a (left) and 1c (right)

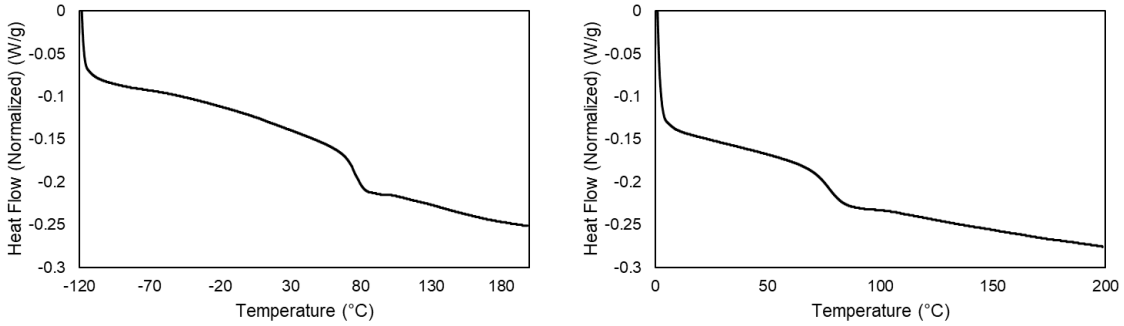

Fig. S103 DSC (2nd heating curve) of Table S5, Entry 2a (left) and 2b (right)

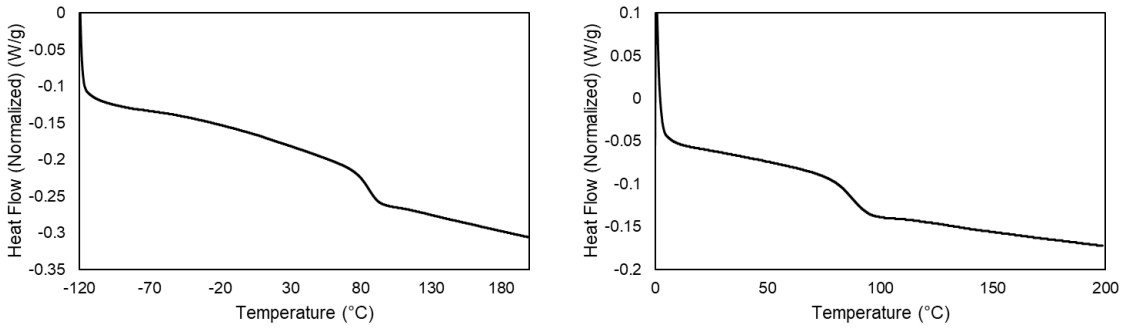

Fig. S104 DSC (2nd heating curve) of Table S5, Entry 3a (left) and 3c (right)

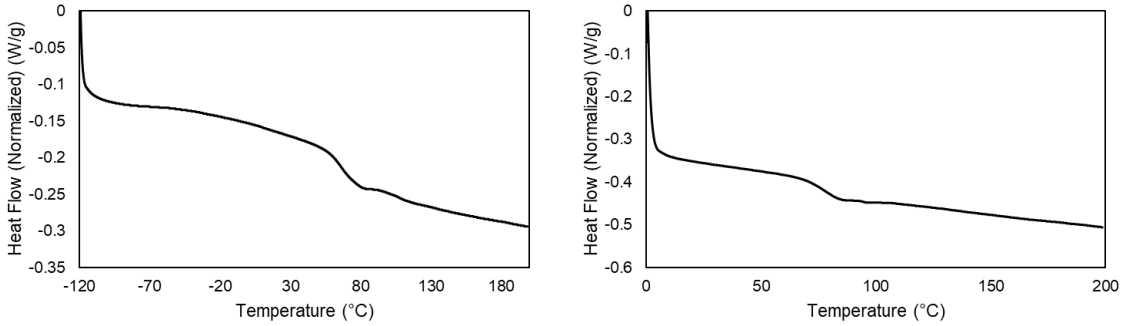

Fig. S105 DSC (2nd heating curve) of Table S6, Entry 1a (left) and 1c (right)

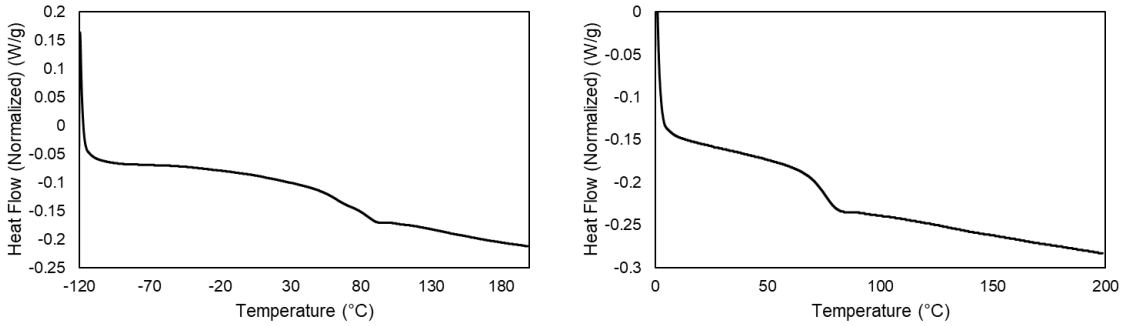

Fig. S106 DSC (2nd heating curve) of Table S6, Entry 2a (left) and 2c (right)

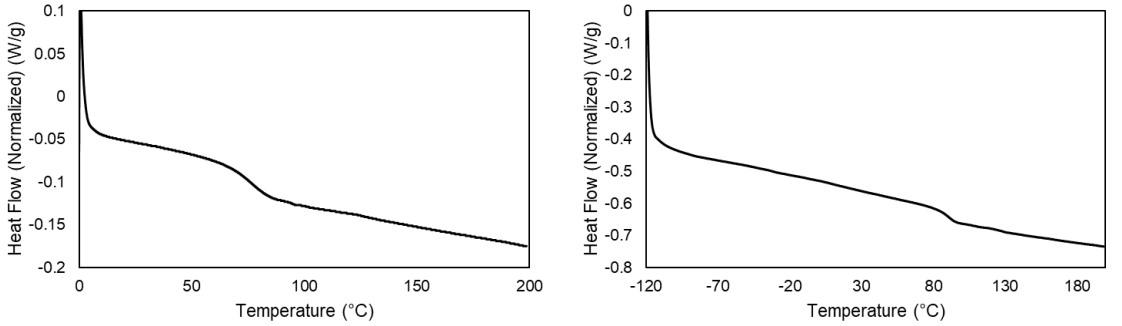

Fig. S107 DSC (2nd heating curve) of Table S6, Entry 3a (left) and 3c (right)

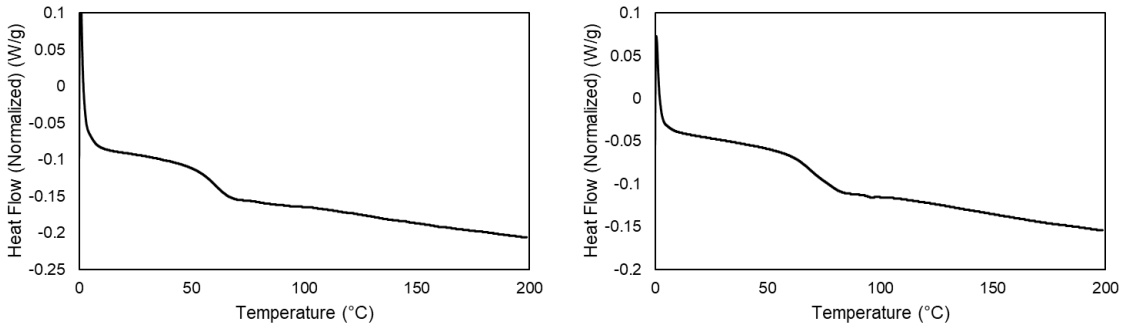

Fig. S108 DSC (2nd heating curve) of Table S7, Entry 1a (left) and 1b (right)

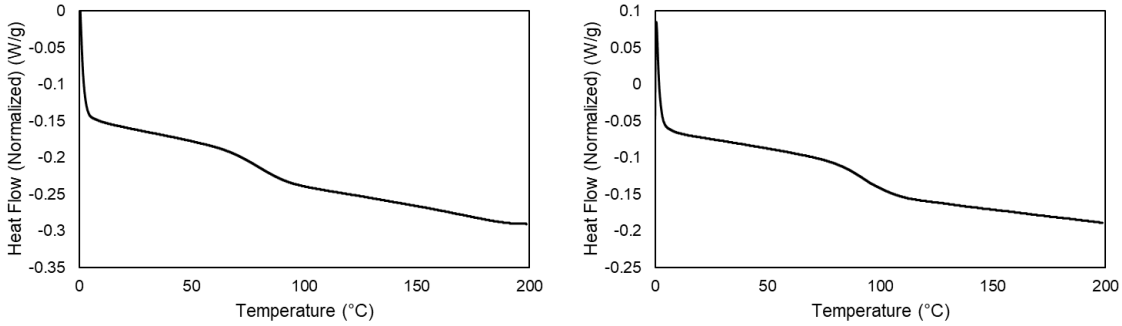

Fig. S109 DSC (2nd heating curve) of Table S7, Entry 2a (left) and 2b (right)

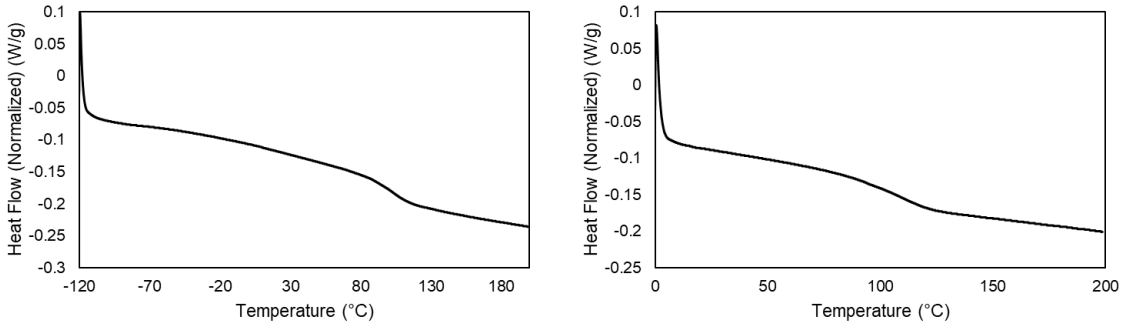

Fig. S110 DSC (2nd heating curve) of Table S7, Entry 3a (left) and 3b (right)

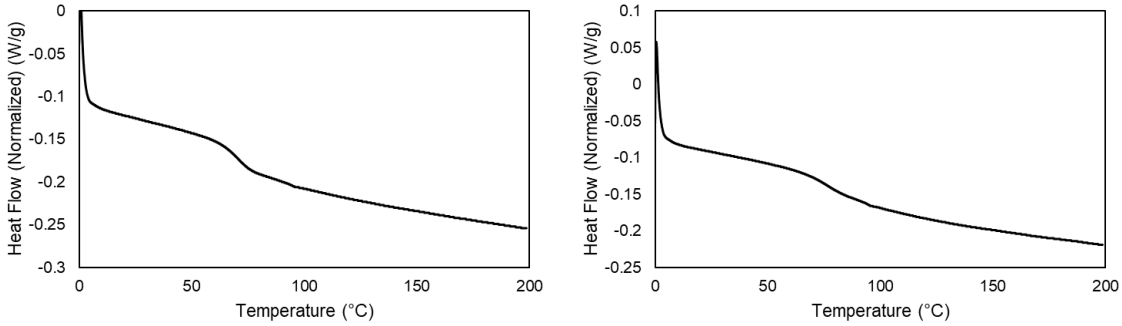

Fig. S111 DSC (2nd heating curve) of Table S8, Entry 1a (left) and 1b (right)

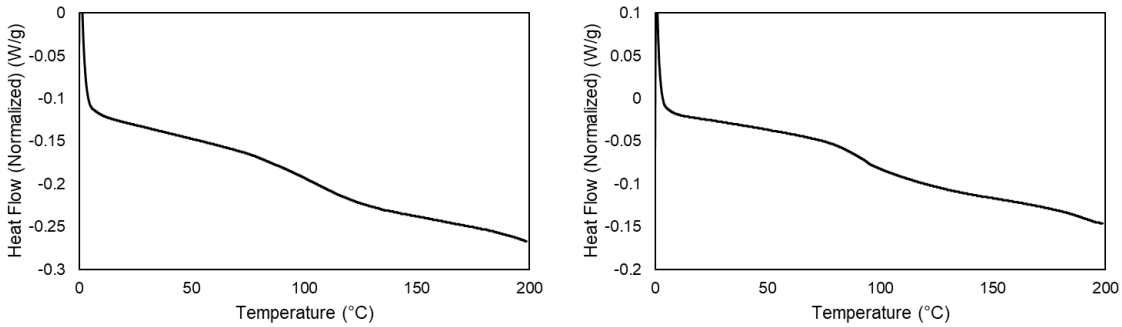

Fig. S112 DSC (2nd heating curve) of Table S8, Entry 2a (left) and 2b (right)

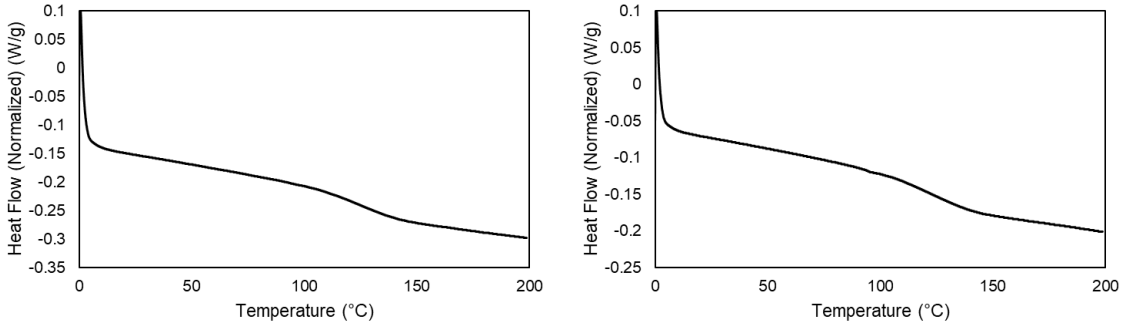

Fig. S113 DSC (2nd heating curve) of Table S8, Entry 3a (left) and 3b (right)

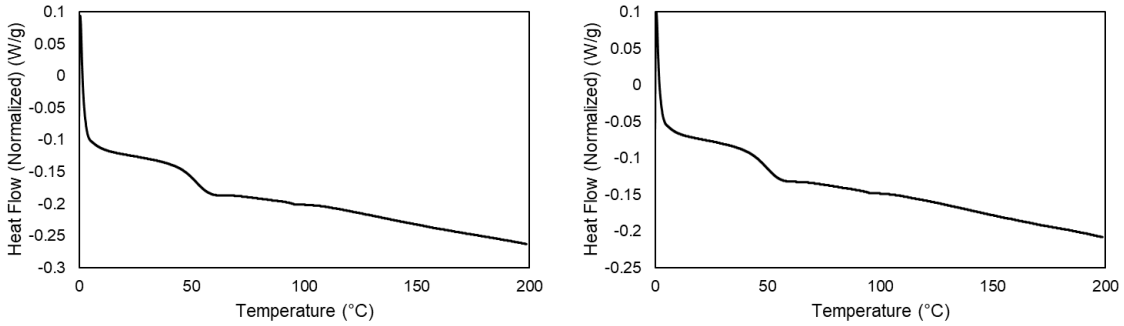

Fig. S114 DSC (2nd heating curve) of Table S9, Entry 1a (left) and 1b (right)

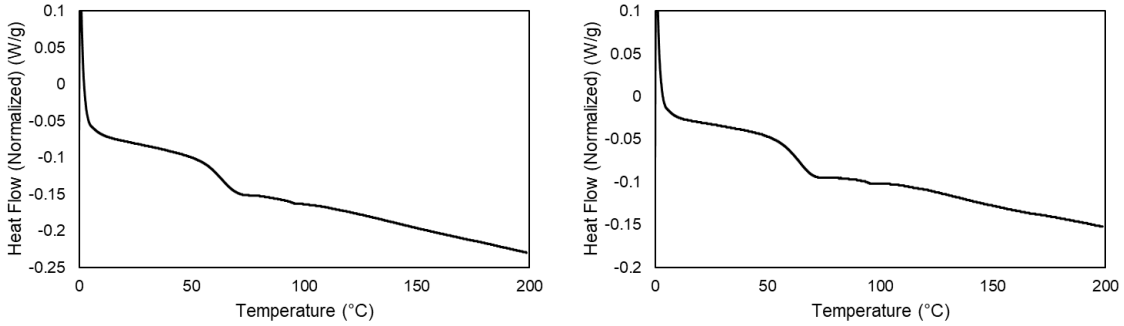

Fig. S115 DSC (2nd heating curve) of Table S9, Entry 2a (left) and 2b (right)

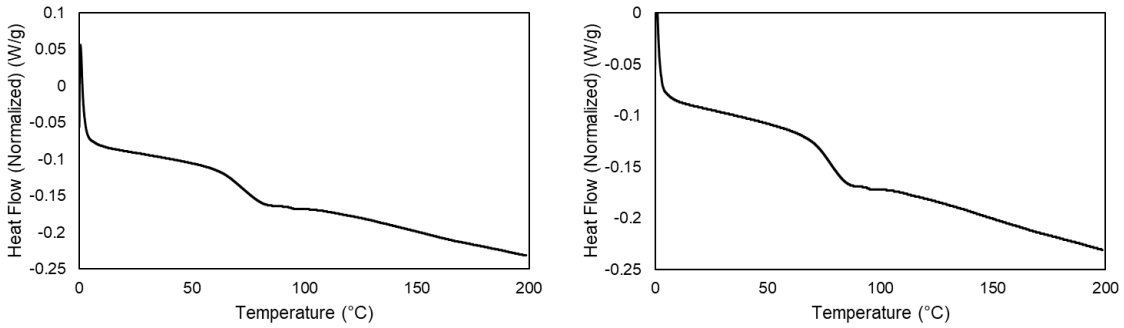

Fig. S116 DSC (2nd heating curve) of Table S9, Entry 3a (left) and 3b (right)

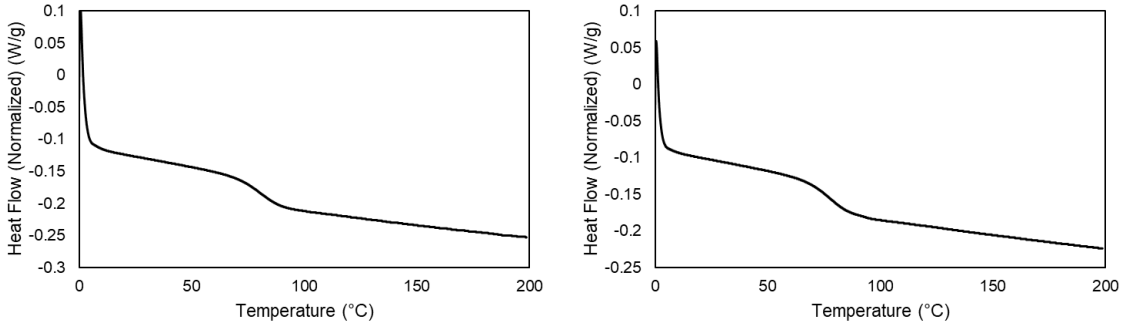

Fig. S117 DSC (2nd heating curve) of Table S10, Entry 1a (left) and 1b (right)

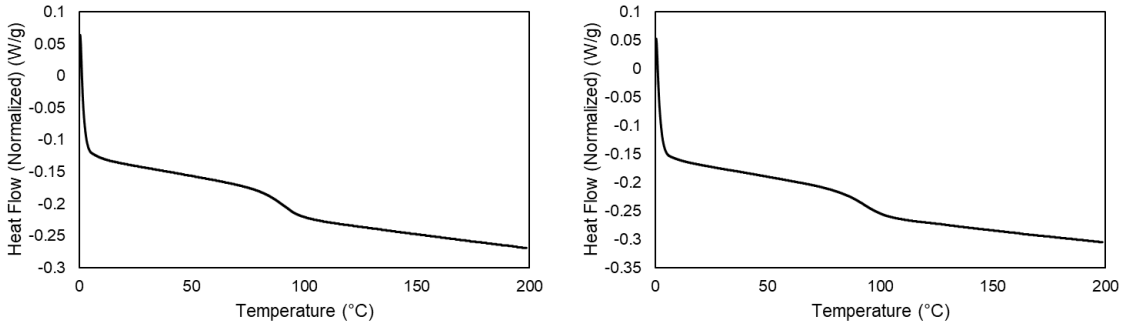

Fig. S118 DSC (2nd heating curve) of Table S10, Entry 2a (left) and 2b (right)

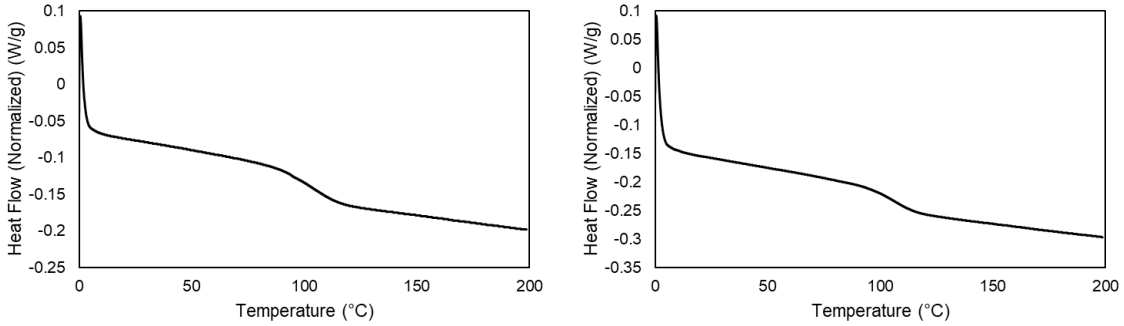

Fig. S119 DSC (2nd heating curve) of Table S10, Entry 3a (left) and 3b (right)

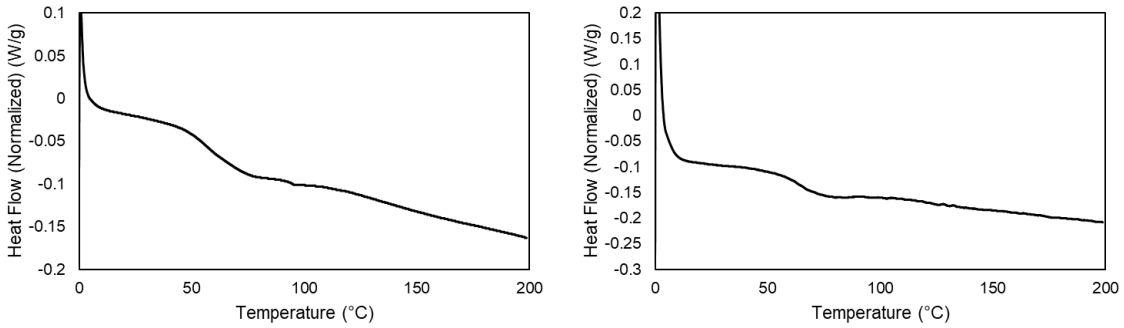

Fig. S120 DSC (2nd heating curve) of Table S10, Entry 4a (left) and 4b (right)

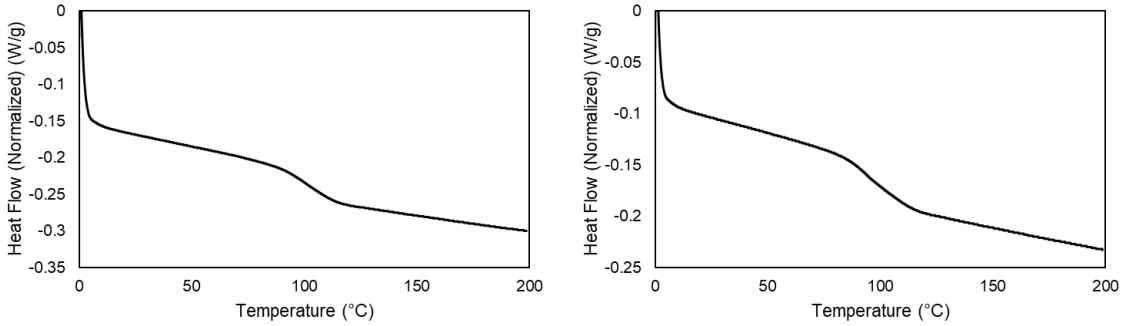

Fig. S121 DSC (2nd heating curve) of Table S10, Entry 5a (left) and 5b (right)

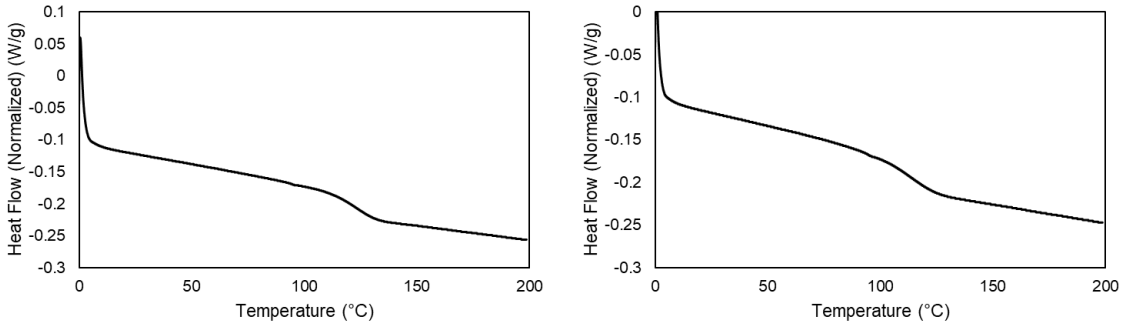

Fig. S122 DSC (2nd heating curve) of Table S10, Entry 6a (left) and 6b (right)

7. Thermogravimetric Analysis (TGA)

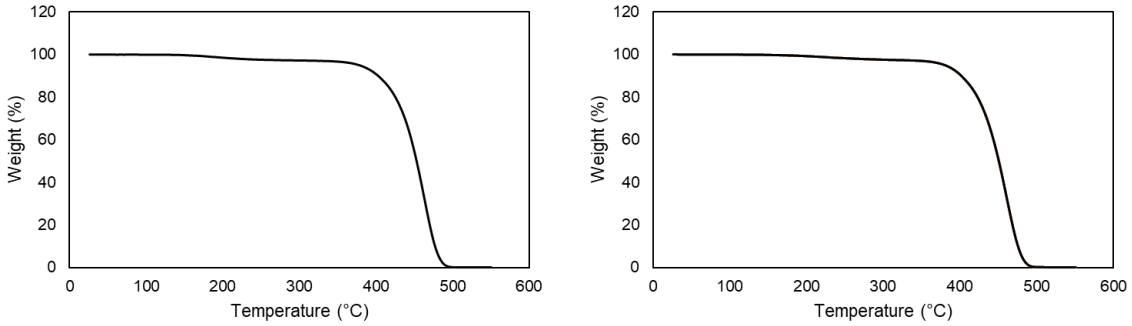

Fig. S123 TGA heating curve of Table S3, Entry 1b (left) and 2c (right)

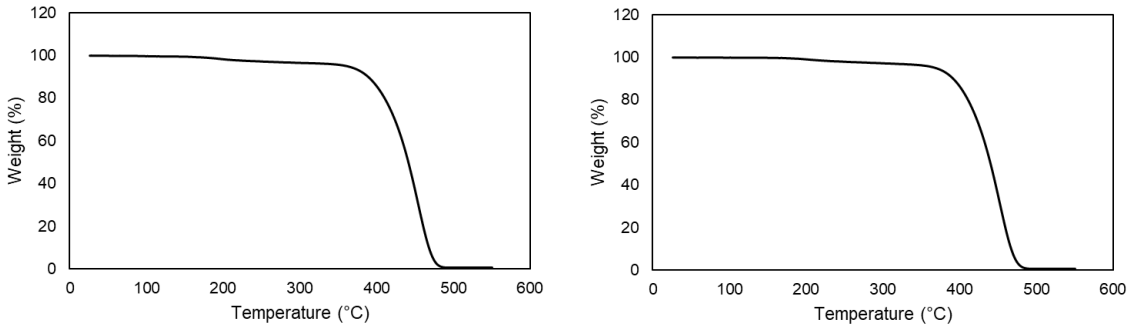

Fig. S124 TGA heating curve of Table S5, Entry 1b (left) and 2b (right)

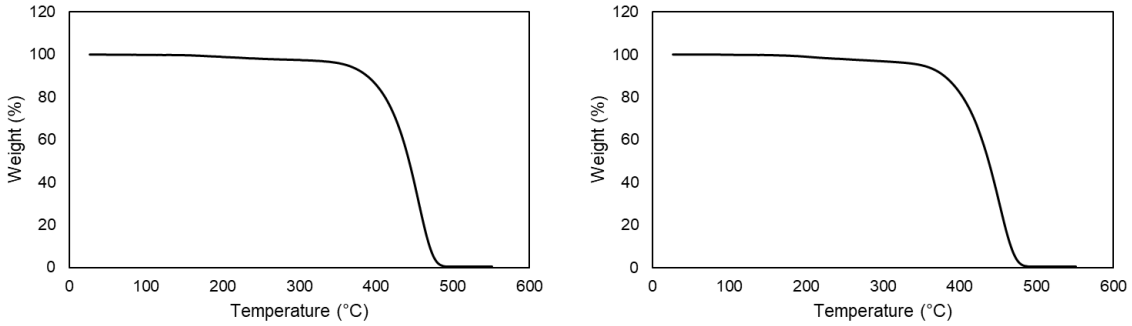

Fig. S125 TGA heating curve of Table S6, Entry 1b (left) and 2c (right)

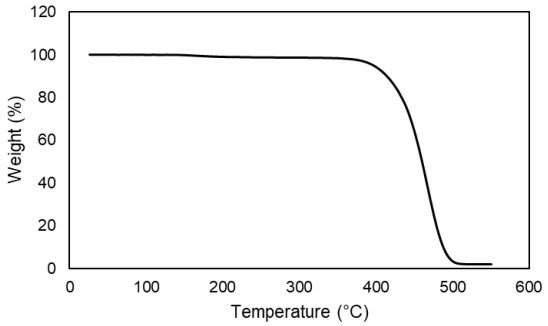

Fig. S126 TGA heating curve of Table S8, Entry 3a

8. Computational Details

Identifying if TMDS could contribute two hydrides

Replacement of the first hydride in TMDS with a chloride from PVC substrate (2-chloropropane) occurs from State 1 to 4. Although, the net energy change from 1 to 4 is negative suggesting thermodynamic feasibility of this replacement, the energy change from 3 to 4 is slightly uphill. States 5 to 8 represent the replacement of second hydride within the same TMDS with a chloride from another PVC molecule. As in case of the first hydride replacement, the net energy change for second replacement is negative with the final step of chloride abstraction (7 to 8) being slightly uphill. Thus, it may be energetically feasible for TMDS to donate both of its hydrides and dechlorinate two C-Cl bonds in PVC.

state 1

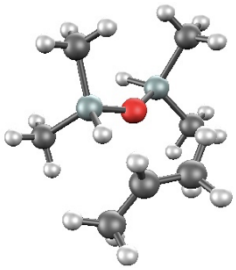

state 2

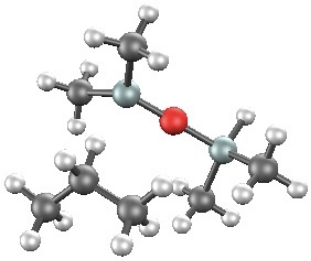

state 3

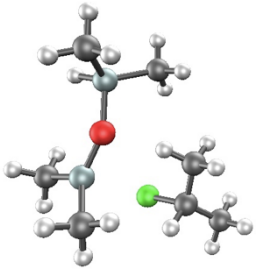

state 4

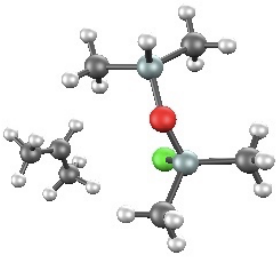

state 8

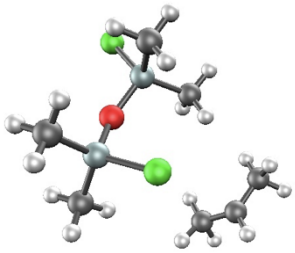

state 7

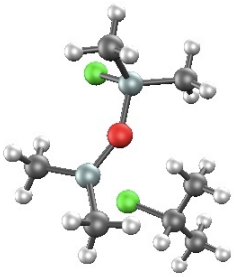

state 6

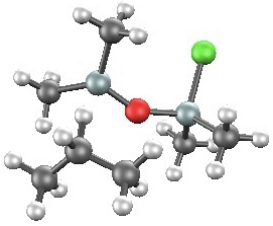

state 5

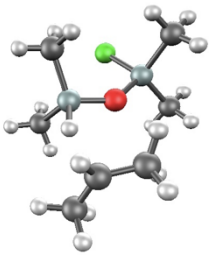

Table S11 Relative free energies of states representing hydride transfer from TMDS to the model propyl cation/2-chloropropane (2CP) and their diagrammatic representations. TMDS_x_x is TMDS where x represents the bond to Si either H or Cl, TMDS_cation represents a Si^+ formed in the TMDS.

States	Constituent species	ΔG (kJ/mol)
1	Isopropyl cation + TMDS_H_H + 2*2CP	0.00
2	propane + TMDS_cation + 2*2CP	-85.40
3	TMDS_cation + 2*2CP + propane	-119.07
4	Isopropyl cation + TMDS_H_Cl + propane + 2CP	-113.29
5	Isopropyl cation + TMDS_H_Cl + propane +2CP	-161.15
6	TMDS_cation + 2*propane + 2CP	-234.80
7	TMDS_cation + 2CP + 2*propane	-264.24
8	TMDS_Cl_Cl + isopropyl cation + 2*propane	-261.91

Comparing Hydrodechlorination with Inter- and Intramolecular Friedel Crafts Alkylation

Table S12 Free energy changes associated with hydride addition, FC alkylation, and polyindene formation upon dechlorination of model PVC compounds.

States	Constituent species	ΔG (kJ/mol)
REF	REF + 2*benzene + 2*($HSiEt_3$)	0.00
Ph	Ph + $HSiEt_3$ + Et_3Si^+ + benzene + H_2	-103.69
H	H + $HSiEt_3$ + Et_3Si^+ + 2*benzene	-153.6
Ph,Ph	Ph,Ph + $ClSiEt_3$ + 2*H_2 + Et_3Si^+	-222.22
POLY	POLY + 2* H_2 + Et_3Si^+ + $ClSiEt_3$ + Benzene	-231.11
H,Ph	H,Ph + $ClSiEt_3$ + Et_3Si^+ + benzene + H_2	-267.19
Ph,H	Ph,H + $ClSiEt_3$ + Et_3Si^+ + benzene + H_2	-273.48
H,H	H,H + $ClSiEt_3$ + Et_3Si^+ + 2*benzene	-313.83

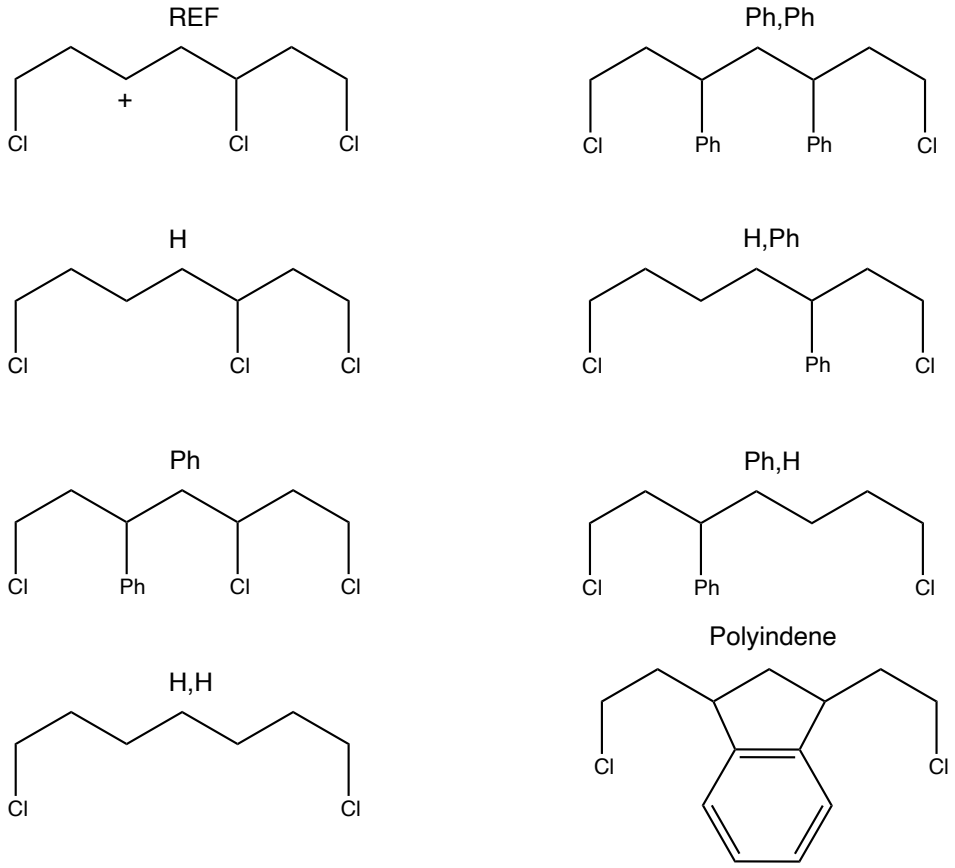

Fig. S127 Structures constituting states described on Fig. 4 of the paper and Table S12 of the SI.

9. References

[1] E. Epifanovsky, A. T. B. Gilbert, X. Feng, J. Lee, Y. Mao, N. Mardirossian, P. Pokhilko, A. F. White, M. P. Coons, A. L. Dempwolff, Z. Gan, D. Hait, P. R. Horn, L. D. Jacobson, I. Kaliman, J. Kussmann, A. W. Lange, K. U. Lao, D. S. Levine, J. Liu, S. C. McKenzie, A. F. Morrison, K. D. Nanda, F. Plasser, D. R. Rehn, M. L. Vidal, Z.-Q. You, Y. Zhu, B. Alam, B. J. Albrecht, A. Aldossary, E. Alguire, J. H. Andersen, V. Athavale, D. Barton, K. Begam, A. Behn, N. Bellonzi, Y. A. Bernard, E. J. Berquist, H. G. A. Burton, A. Carreras, K. Carter-Fenk, R. Chakraborty, A. D. Chien, K. D. Closser, V. Cofer-Shabica, S. Dasgupta, M. de Wergifosse, J. Deng, M. Diedenhofen, H. Do, S. Ehlert, P.-T. Fang, S. Fatehi, Q. Feng, T. Friedhoff, J. Gayvert, Q. Ge, G. Gidofalvi, M. Goldey, J. Gomes, C. E. González-Espinoza, S. Gulania, A. O. Gunina, M. W. D. Hanson-Heine, P. H. P. Harbach, A. Hauser, M. F. Herbst, M. Hernández Vera, M. Hodecker, Z. C. Holden, S. Houck, X. Huang, K. Hui, B. C. Huynh, M. Ivanov, Á. Jász, H. Ji, H. Jiang, B. Kaduk, S. Kähler, K. Khistyaev, J. Kim, G. Kis, P. Klunzinger, Z. Koczor-Benda, J. H. Koh, D. Kosenkov, L. Koulias, T. Kowalczyk, C. M. Krauter, K. Kue, A. Kunitsa, T. Kus, I. Ladjánszki, A. Landau, K. V. Lawler, D. Lefrancois, S. Lehtola, R. R. Li, Y.-P. Li, J. Liang, M. Liebenthal, H.-H. Lin, Y.-S. Lin, F. Liu, K.-Y. Liu, M. Loipersberger, A. Luenser, A. Manjanath, P. Manohar, E. Mansoor, S. F. Manzer, S.-P. Mao, A. V. Marenich, T. Markovich, S. Mason, S. A. Maurer, P. F. McLaughlin, M. F. S. J. Menger, J.-M. Mewes, S. A. Mewes, P. Morgante, J. W. Mullinax, K. J. Oosterbaan, G. Paran, A. C. Paul, S. K. Paul, F. Pavošević, Z. Pei, S. Prager, E. I. Proynov, Á. Rák, E. Ramos-Cordoba, B. Rana, A. E. Rask, A. Rettig, R. M. Richard, F. Rob, E. Rossomme, T. Scheele, M. Scheurer, M. Schneider, N. Sergueev, S. M. Sharada, W. Skomorowski, D. W. Small, C. J. Stein, Y.-C. Su, E. J.

Sundstrom, Z. Tao, J. Thirman, G. J. Tornai, T. Tsuchimochi, N. M. Tubman, S. P. Veccham, O. Vydrov, J. Wenzel, J. Witte, A. Yamada, K. Yao, S. Yeganeh, S. R. Yost, A. Zech, I. Y. Zhang, X. Zhang, Y. Zhang, D. Zuev, A. Aspuru-Guzik, A. T. Bell, N. A. Besley, K. B. Bravaya, B. R. Brooks, D. Casanova, J.-D. Chai, S. Coriani, C. J. Cramer, G. Cserey, A. E. DePrince, R. A. DiStasio, A. Dreuw, B. D. Dunietz, T. R. Furlani, W. A. Goddard, S. Hammes-Schiffer, T. Head-Gordon, W. J. Hehre, C.-P. Hsu, T.-C. Jagau, Y. Jung, A. Klamt, J. Kong, D. S. Lambrecht, W. Liang, N. J. Mayhall, C. W. McCurdy, J. B. Neaton, C. Ochsenfeld, J. A. Parkhill, R. Peverati, V. A. Rassolov, Y. Shao, L. V. Slipchenko, T. Stauch, R. P. Steele, J. E. Subotnik, A. J. W. Thom, A. Tkatchenko, D. G. Truhlar, T. Van Voorhis, T. A. Wesolowski, K. B. Whaley, H. L. Woodcock, P. M. Zimmerman, S. Faraji, P. M. W. Gill, M. Head-Gordon, J. M. Herbert and A. I. Krylov, *J. Chem. Phys.,* 2021, **155**, 084801.

[2] J.-D. Chai and M. Head-Gordon, *Phys. Chem. Chem. Phys.* 2008, **10**, 6615-6620.

[3] J.-D. Chai and M. Head-Gordon, *J. Chem. Phys.* 2008, **128**, 084106.

[4] T. N. Truong and E. V. Stefanovich, *Chem. Phys. Lett.* 1995, **240**, 253-260.

[5] V. Barone and M. Cossi, *J. Phys. Chem. A* 1998, **102**, 1995-2001.

[6] M. Cossi, N. Rega, G. Scalmani and V. Barone, *J. Comput. Chem.* 2003, **24**, 669-681.

[7] McQuarrie, D. A. Ideal polyatomic gas, In *Statistical Mechanics*, University Science Books, pp. 129-141.